

LEVEL



DAVID W. TAYLOR NAVAL SHIP
RESEARCH AND DEVELOPMENT CENTER

Bethesda, Maryland 20084

FRICTIONAL CHARACTERISTICS OF TILT-PAD
AND SWING-PAD THRUST BEARINGS

by

Nathan T. Sides
Thomas L. Daugherty

DTIC
SELECTED
NOV 21 1980

APPROVED FOR PUBLIC RELEASE: DISTRIBUTION UNLIMITED

SHIP MATERIALS ENGINEERING DEPARTMENT
RESEARCH AND DEVELOPMENT REPORT

September 1980

DTNSRDC-80/101

AD A091909

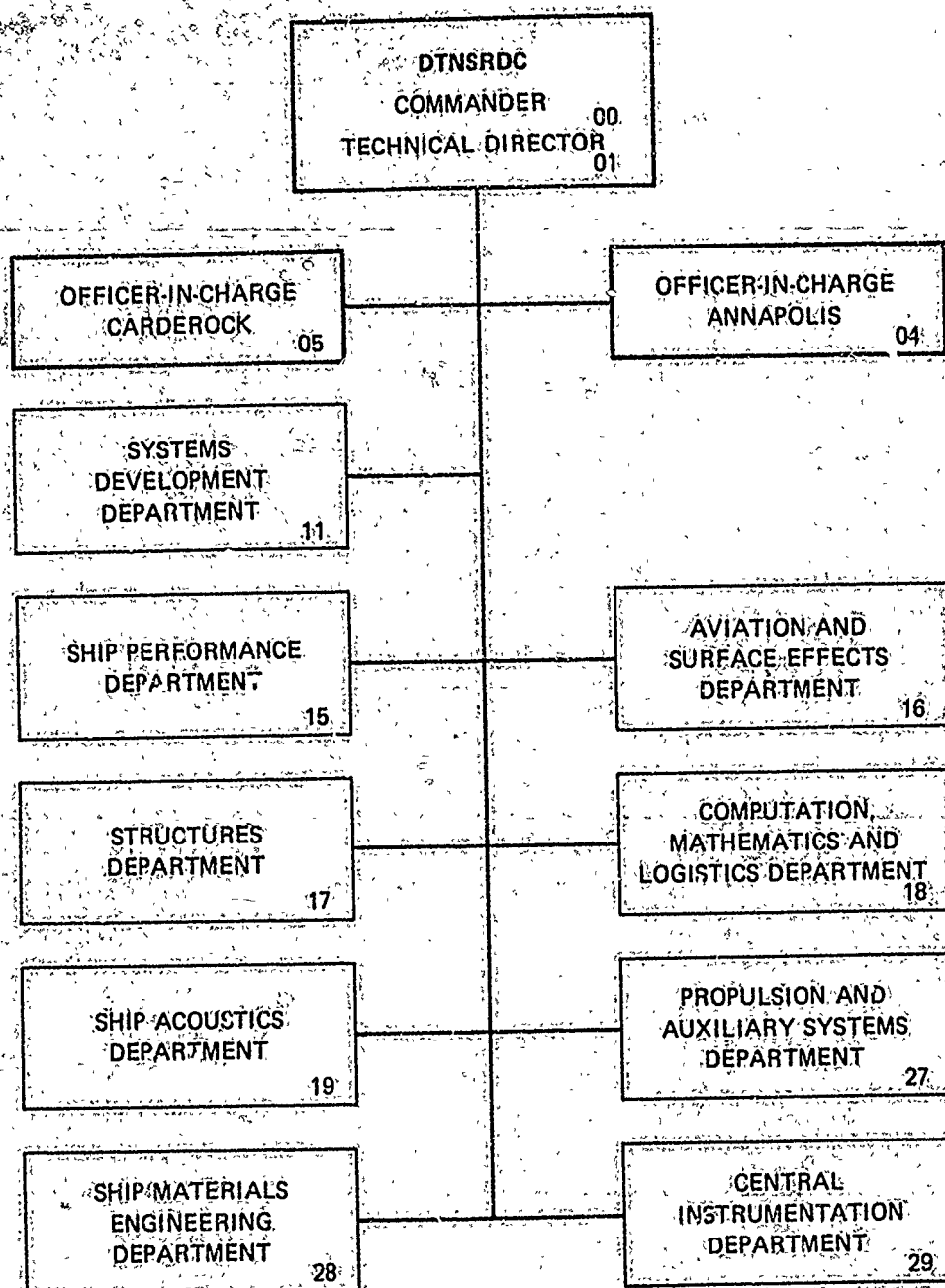
FRICTIONAL CHARACTERISTICS OF TILT-PAD
AND SWING-PAD THRUST BEARINGS

DDG FILE COPY

DTNSRDC-80/101

8C11 17 005

MAJOR DTNSRDC ORGANIZATIONAL COMPONENTS



DTNSRDC ISSUES THREE TYPES OF REPORTS

1. DTNSRDC REPORTS, A FORMAL SERIES, CONTAIN INFORMATION OF PERMANENT TECHNICAL VALUE. THEY CARRY A CONSECUTIVE NUMERICAL IDENTIFICATION REGARDLESS OF THEIR CLASSIFICATION OR THE ORIGINATING DEPARTMENT.

2. DEPARTMENTAL REPORTS, A SEMIFORMAL SERIES, CONTAIN INFORMATION OF A PRELIMINARY, TEMPORARY, OR PROPRIETARY NATURE OR OF LIMITED INTEREST OR SIGNIFICANCE. THEY CARRY A DEPARTMENTAL ALPHANUMERICAL IDENTIFICATION.

3. TECHNICAL MEMORANDA, AN INFORMAL SERIES, CONTAIN TECHNICAL DOCUMENTATION OF LIMITED USE AND INTEREST. THEY ARE PRIMARILY WORKING PAPERS INTENDED FOR INTERNAL USE. THEY CARRY AN IDENTIFYING NUMBER WHICH INDICATES THEIR TYPE AND THE NUMERICAL CODE OF THE ORIGINATING DEPARTMENT. ANY DISTRIBUTION OUTSIDE DTNSRDC MUST BE APPROVED BY THE HEAD OF THE ORIGINATING DEPARTMENT ON A CASE-BY-CASE BASIS.

(16) S'0923/

UNCLASSIFIED

SECURITY CLASSIFICATION OF THIS PAGE (When Data Entered)

REPORT DOCUMENTATION PAGE		READ INSTRUCTIONS BEFORE COMPLETING FORM
1. REPORT NUMBER	2. GOVT ACCESSION NO.	3. RECIPIENT'S CATALOG NUMBER
(14) DTNSRDC-80/101	AD-A091909	(9)
4. TITLE (and Subtitle)		5. TYPE OF REPORT & PERIOD COVERED
(6) FRICTIONAL CHARACTERISTICS OF TILT-PAD AND SWING-PAD THRUST BEARINGS		Research and Development report
6. PERFORMING ORG. REPORT NUMBER		
7. AUTHOR(s)		8. CONTRACT OR GRANT NUMBER(s)
(10) Nathan T. Sides Thomas L. Daugherty		
9. PERFORMING ORGANIZATION NAME AND ADDRESS		10. PROGRAM ELEMENT, PROJECT, TASK AREA & WORK UNIT NUMBERS
David W. Taylor Naval Ship R&D Center Bethesda, MD 20084		See reverse side.
11. CONTROLLING OFFICE NAME AND ADDRESS		12. REPORT DATE
Naval Sea Systems Command (NAVSEA 05DC3) Washington, DC 20362		(11) Sep 1980
14. MONITORING AGENCY NAME & ADDRESS (if different from Controlling Office)		13. NUMBER OF PAGES
(12) 46		44
		15. SECURITY CLASS. (of this report)
		UNCLASSIFIED
		15a. DECLASSIFICATION/DOWNGRADING SCHEDULE
16. DISTRIBUTION STATEMENT (of this Report)		
APPROVED FOR PUBLIC RELEASE; DISTRIBUTION UNLIMITED		
17. DISTRIBUTION STATEMENT (of the abstract entered in Block 20, if different from Report)		
18. SUPPLEMENTARY NOTES		
19. KEY WORDS (Continue on reverse side if necessary and identify by block number)		
Bearing Thrust Bearing Friction Hydrodynamic Lubrication		
20. ABSTRACT (Continue on reverse side if necessary and identify by block number)		
<p>This report presents frictional performance of oil-lubricated thrust bearings of conventional tilt-pad and swing-pad designs. Results from the conventional tilt-pad bearing are used as a baseline. All tests were conducted at a fixed speed and temperature, while load was varied. All bearings were tested with the pad surfaces in the centered and off-centered positions. Friction</p> <p>(Continued on reverse side)</p>		

DTIC
ELECTE
NOV 21 1980

DD FORM 1 JAN 73 1473

EDITION OF 1 NOV 65 IS OBSOLETE
S/N 0102-LF-014-6601

UNCLASSIFIED
SECURITY CLASSIFICATION OF THIS PAGE (When Data Entered)

387682

LM

UNCLASSIFIED

SECURITY CLASSIFICATION OF THIS PAGE (When Data Entered)

Block 10

Program Element 63561N

Task Area S0 923 001

Task 21257

Work Unit 1102-016

Block 20 continued

results in the hydrodynamic region compared favorably with conventional hydrodynamic theory. The hydrodynamic load capacities of the centered swing-pad bearing designs were 25 to 80 percent higher than that of the centered tilt-pad bearing. Improvements in performance were observed in the regions of hydrodynamic and mixed lubrication by off-setting the pad surfaces for both the tilt-pad and the elastomeric swing-pad designs. Breakaway friction of the laminated elastomeric swing-pad design was about 50 percent higher than that measured for either the conventional tilt-pad or hybrid-pad bearing designs.

Accession For	
NTIS GRA&I	<input checked="checked" type="checkbox"/>
DTIC T'B	<input type="checkbox"/>
Unannounced	<input type="checkbox"/>
Justification	
By	
Distribution/	
Availability Codes	
Dist	Avail and/or Special
A	

UNCLASSIFIED

SECURITY CLASSIFICATION OF THIS PAGE (When Data Entered)

TABLE OF CONTENTS

	Page
LIST OF FIGURES.	iii
LIST OF TABLES	iv
LIST OF ABBREVIATIONS.	v
LIST OF SYMBOLS.	vi
ABSTRACT	1
ADMINISTRATIVE INFORMATION	1
INTRODUCTION	1
APPROACH	2
THEORETICAL BASIS.	2
TILT-PAD BEARING	4
SWING-PAD BEARING.	5
EQUIPMENT, MATERIALS, AND PROCEDURES	6
BEARINGS TESTED.	8
RESULTS.	9
DISCUSSION	13
CONCLUSIONS.	14
FUTURE PLANS	15
REFERENCES	37

LIST OF FIGURES

1 - Hydrodynamic Converging Tapered Wedge.	16
2 - Shoe Dimensions.	17
3 - Typical Tilt-Pad Thrust Bearing Assembly	18
4 - Pressure Distribution on Tilt-Pad Bearing.	19

	Page
5 - Swing-Pad Bearing, Centered.	20
6 - Pressure Distribution of Swing-Pad Bearing	21
7 - Hybrid-Pad Bearing	22
8 - Centered and Offset Swing-Pad Bearing.	23
9 - Test Machine	24
10 - Test Bearing in Oil Tank	25
11 - Test Machine Schematic	26
12 - Tilt-Pad Assembly, Centered (After test)	27
13 - Swing-Pad Assembly, Centered	28
14 - Hybrid-Pad Assembly, Centered.	29
15 - Results, Tilt-Pad, Centered.	30
16 - Results, Tilt-Pad, Offset.	31
17 - Results, Swing-Pad, Centered	32
18 - Results, Swing-Pad, Offset	33
19 - Results, Hybrid-Pad, Centered.	34
20 - Results, Hybrid-Pad, Offset.	35
21 - Superimposed Plots	36

LIST OF TABLES

1 - Last Hydrodynamic Values.	10
2 - Last Transition Zone Values From Hydrodynamic to Mixed Lubrication	11
3 - Breakaway Coefficient of Friction.	12

LIST OF ABBREVIATIONS

$^{\circ}\text{C}$	Degrees Celsius
$^{\circ}\text{F}$	Degrees Fahrenheit
cm	Centimeter
ft	Foot
in.	Inch
in./s	Inches per second
kPa	Kilopascal
lb	Pound
lb-ft	Pound-foot
lb-in.	Pound-inch
m	Meter
min	Minute
mm	Millimeter
m/s	Meter per second
N	Newton
Nm	Newton-meter
psi	Pounds per square inch
rpm	Revolutions per minute
rms	Root mean square
s	Second
$\mu\text{in.}$	Microinch
μm	Micrometer

LIST OF SYMBOLS

a	(h_i/h_o)
B	Bearing pad circumferential length, cm (in.)
b	Bearing pad radial length, cm (in.)
d	Moment arm from P_r to pad centerline, cm (in.)
F	Friction force, N (lb)
F_f	Force due to friction, N (lb)
f	Coefficient of friction
h_i	Lubricant film thickness at leading edge, mm (in.)
h_o	Lubricant minimum film thickness at trailing edge, mm (in.)
K_f	Function of η
K_p	Function of η
M_f	Moment due to friction force, Nm (lb-in.)
M_p	Moment due to pressure forces, Nm (lb-in.)
P_{avg}	Average load on bearing surface, kPa (psi)
P_r	Resultant pressure vector, N (lb)
R	Radius of swing, cm (in.)
U	Surface speed, m/s (in./s)
W	Total bearing applied load, N (lb)
x	Distance from pad leading edge to pivot point, cm (in.)
η	Modifying factor
μ	Absolute viscosity, poise (reyns)

ABSTRACT

This report presents frictional performance of oil-lubricated thrust bearings of conventional tilt-pad and swing-pad designs. Results from the conventional tilt-pad bearing are used as a baseline. All tests were conducted at a fixed speed and temperature, while load was varied. All bearings were tested with the pad surfaces in the centered and off-centered positions. Friction results in the hydrodynamic region compared favorably with conventional hydrodynamic theory. The hydrodynamic load capacities of the centered swing-pad bearing designs were 25 to 80 percent higher than that of the centered tilt-pad bearing. Improvements in performance were observed in the regions of hydrodynamic and mixed lubrication by off-setting the pad surfaces for both the tilt-pad and the elastomeric swing-pad designs. Breakaway friction of the laminated elastomeric swing-pad design was about 50 percent higher than that measured for either the conventional tilt-pad or hybrid-pad bearing designs.

ADMINISTRATIVE INFORMATION

This report covers work conducted for the Naval Sea Systems Command (NAVSEA 05DC3; formerly NAVSEA 6113) under Research, Development, Test and Evaluation Funds, Work Request 9G002, Work Unit 1102-016.

INTRODUCTION

A primary goal of the U.S. Navy's Improved Performance Machinery Program is to reduce the size and weight of the steam propulsion plant and associated equipment in submarines. Such reductions are explored herein for an oil-lubricated main thrust bearing. A basic requirement for an improved bearing is increased load capacity. The potential for increased load capacity was demonstrated in exploratory tests^{1*} conducted on a bearing design called the "swing-pad bearing," which was invented at David W. Taylor Naval Ship Research and Development Center (DTNSRDC), patent number 3,930,691 of 6 Jan 1976. This report includes comparison of the frictional characteristics and load carrying capacity between two variations of the swing-pad bearing and the conventional tilt-pad bearing.

*References are listed on page 37.

APPROACH

Friction in hydrodynamic sliding surface bearings is a function of the viscosity of the lubricant, surface speed of the bearing, applied load, and the size of the bearing pad. The friction of thrust bearings of tilt-pad and swing-pad designs was measured on the same test machine and compared over a range of applied bearing loads. The tilt-pad bearing, purchased commercially, was used as a reference. Two swing-pad bearing designs were evaluated. All bearings were tested with the center of tilt or swing centered and offset to one side. Comparison of frictional results was also made with that predicted by existing theoretical analysis.^{2,3,4} The load capacities in the hydrodynamic region and in the mixed lubrication region of each design were compared. Breakaway experiments were conducted for each design and the results compared in this report.

THEORETICAL BASIS

Theoretical analysis of hydrodynamic bearings is based upon existence of a converging wedge such as that shown in Figure 1. Hydrodynamic theory applied to a tapered wedge gives the following equations, according to Fuller²

$$h_o = \left(\frac{6\mu UB\eta K_p}{P_{avg}} \right)^{1/2} \quad (1)$$

$$F = \mu bBK_f \frac{U}{h_o} \quad (2)$$

$$f = \frac{F}{W} \quad (3)$$

For the purposes of this investigation, the following values apply (see Figure 2)

$$B = 3.18 \text{ cm (1.25 in.)}$$

$$b = 2.97 \text{ cm (1.17 in.)}$$

$$\frac{b}{l} \approx 1, \text{ therefore, } \eta = 0.44$$

Assuming the leading edge film thickness to be twice the trailing edge film thickness, $a = 2$, $K_p = 0.0265$, and $K_f = 0.773$
from (3) /

$$f = \frac{F}{PbB} \quad (4)$$

combining Equations (1), (2), and (4)

$$f = \frac{\mu b B K_f U}{\left(\frac{6 \mu U B \eta K_p}{P_{avg}} \right)^{1/2}} \cdot \frac{1}{PbB} \quad (5)$$

Simplifying and applying numerical values,

$$f = 2.9 \left(\frac{\mu U}{PB} \right)^{1/2} \quad (6)$$

When plotted on log-log graph paper, the above expression yields a straight line. Simplifying Equation (1), the following expression is obtained for the minimum film thickness

$$h_o = 0.264 \left(\frac{\mu U B}{P} \right)^{1/2} \quad (7)$$

Hydrodynamic lubrication is said to exist as long as the bearing behaves according to the above expressions. Full fluid separation exists between the bearing and the mating runner surface and the only frictional losses are due to fluid shear. Under these conditions, virtually no wear occurs and bearing life is theoretically infinite. The coefficient of friction decreases in proportion to the parameter $(\mu U/Pb)^{1/2}$. Load is supported entirely by pressurized lubricant.

In practice, however, a limit to hydrodynamic lubrication exists. As the parameter $\mu U/Pb$ is decreased through increased load, decreased speed or viscosity of the lubricant, the minimum film thickness of the lubricant is also reduced. A point is reached when the height of the asperities on the bearing and runner surfaces exceeds the thickness of the fluid film and intermittent contact occurs. The coefficient of friction will continue to decrease to a minimum value. The slope will depart from the straight line observed in the hydrodynamic region. Continued decreases in $\mu U/Pb$ will produce a sudden increase in the coefficient of friction. This transitional region of operation, characterized by load being shared by both asperity contacts and pressurized lubricant, is referred to as "mixed lubrication."

Further reduction in $\mu U/Pb$ leads to further deterioration to the point that load is completely supported by surface-to-surface contact where the lubricant no longer separates the bearing and runner. The coefficient of friction will then be large and reflect the frictional properties of the mating materials. This condition is known as "boundary lubrication."

TILT-PAD BEARING

The conventional tilt-pad thrust bearing consists of individual pads usually ranging in number from two to twelve and spaced annularly as shown in Figure 3. It consists of a flat sliding surface, or runner, sliding over the pads which are free to pivot or tilt independently. The pads are usually completely immersed in the lubricant. The tilt-pad thrust bearing was invented by Albert Kingsbury and A.G.M. Michell in the early 1900s.

The basic theory behind the tilt-pad design is that the pivot shoe is free to adjust itself to the optimum angle for any operating condition. Its basic load capacity is derived by creation of a converging wedge of lubricant in the direction of motion. Behavior is similar to that discussed in the theoretical basis section of this report. The pivot location may be moved to various positions across the

width of the pad. The center of pressure must be located at the pivot position to achieve equilibrium⁵ (see Figure 4). A centrally pivoted bearing allows operation in both directions of rotation. From a theoretical standpoint, however, a flat-surfaced, centrally pivoted bearing with constant lubricant viscosity has zero load-carrying capacity.⁶

In practice, it has been found that centrally pivoted pads have significant load-carrying capacity. The explanation^{6,7,8} for this paradox is that load-carrying capacity is produced by two primary effects. First, the change in viscosity of the lubricant generates a finite load-carrying capacity. The viscosity changes as a result of work done upon the lubricant as it passes across the bearing. Second, the shape of the pad surfaces creates a change in the pressure profile and influences the load-carrying capacity. Convex surfaces with a certain amount of curvature offer important advantages. These may be produced in several ways. Some degree of crowning usually results from the manufacturing process used in finishing the pads. Elastic deformations under load result from the single point support of the pressure distribution on the pad surface. Deformations due to thermal gradients in the pad itself may also contribute to crowning.

Assuming rigid flat pad surfaces and constant lubricant viscosity, an expression has been derived⁷ for the location of the center of pressure in terms of the amount of offset. The optimum pivot location is found to correspond to an offset of 0.58 of the length of the bearing, toward the trailing edge.

SWING-PAD BEARING

The swing-pad thrust bearing is designed to be a hydrodynamic bearing and as such is expected to have similar operating conditions to those described earlier. Like the tilt-pad thrust bearing, it consists of a series of individual pads, as shown in Figure 3. One version of the swing-pad thrust bearing is shown in Figure 5 and consists of a set of three spherical, metal shims separated by elastomer laminates. These components are assembled between a mounting base and a surface platform. In contrast to the tilt-pad design, the swing-pad bearing is designed with its center of pivot or "swing" located above the bearing face instead of behind it (see Figure 6). The primary objective of the laminates is to provide high compressive and low shear stiffness. High compressive stiffness is desirable

in practical applications to control and maintain shaft position. Low shear stiffness allows the bearing surface to displace along its swing arc for formation of the desired converging wedge.

An idealized version of the swing-pad bearing can be approximated by minimizing the shear stiffness, while providing very high compressive stiffness. This design is referred to as the "hybrid-pad bearing." It consists of replacing the elastomer and metal, spherical laminates with steel balls which ride between hardened spherical surfaces (see Figure 7).

Note that the center of pressure on the pad surface is not required to pass through the center of swing as was required in the tilt-pad bearing analysis. For example, if the pad surface were offset toward the leading edge (see Figure 8), a significant moment is created by this offset which encourages a converging wedge.

The conventional theory of hydrodynamic sliding surface bearings considers only the pressure loading and location of the center of pressure on the surface of the pads. Drag or friction forces are usually ignored. This is an acceptable procedure when operation is clearly in the hydrodynamic region. However, as operation moves into the transition between hydrodynamic and mixed lubrication, it becomes apparent that the frictional forces play a more significant role. For the tilt-pad bearing with its center of pivot located behind the pad surface, a friction force on the surface produces a moment in a direction opposing desirable converging wedge formation (see Figure 4). For the swing-pad design with its center of swing located above the pad surface, the friction force on the surface produces a moment in the direction of desirable converging wedge formation (see Figure 6). Operation in the hydrodynamic region with the same wedge angle should provide the same performance for both the tilt-pad and swing-pad designs. The range of hydrodynamic lubrication and mixed lubrication would be expected to be extended with proper swing-pad design due to the location of the swing center.

EQUIPMENT, MATERIALS, AND PROCEDURES

The test machine (see Figures 9, 10, and 11) uses a hydraulic drive system coupled to a gearbox capable of bidirectional rotation. Two disk runners are splined on the shaft and are free to move axially in the vertical direction. Two sets of bearing pads, each consisting of three pads located 120 degrees apart, are loaded against the disk runners. The arrangement is very similar to an automobile

disk brake system. Loading is accomplished with hydraulic cylinders. The bearing pads and runner assembly is submerged in a lubricant reservoir. The reservoir is made of plexiglass to allow viewing. A heat exchanger is also incorporated to regulate the bulk lubricant temperature.

Measured parameters are shaft speed, torque (via an in-line torquemeter), load (via load cells and pressure gauges), and bulk lubricant temperature (via a thermocouple).

The runner surfaces used in all tests were mild steel ground and polished circumferentially to a surface finish of 0.10 to 0.20 μm (4 to 8 $\mu\text{in. rms}$ as measured in the direction of rotation. Bearing shoes were made of babbitt of the following composition:

Tin	89.60 percent
Lead	0.14 percent
Antimony	7.99 percent
Copper	2.16 percent

This composition is very similar to ASTM babbitt grade 2 and Navy grade 2.

The babbitt shoes (0.64 cm (0.25 in.) thick) were cemented to the bearing pads. Two steel pins were also used to carry the shear load and maintain the relative position of the shoe to the pad. Two sets of three pads each were mounted on loading rings. The shoes were then manually polished by placing the assembly against a rotating polishing disk. Emery paper of successively finer grades (down to 600 grit) was used on the polishing disk and kept constantly wet to prevent clogging. Rotation of the polishing wheel was always in the same direction as that of the runner disk in the test machine. Surface finishes of 0.1 to 0.15 μm (4 to 6 $\mu\text{in. rms}$) were achieved on the babbitt surfaces in this manner.

The two bearing sets were mounted in the test machine and the shaft rotated at zero load and 35 rpm. Temperature of the lubricant was regulated at 50°C (122°F). The lubricant used was 2190 TEP oil (MIL-L-17331) with a viscosity roughly equivalent to an SAE 20 oil. Load was applied to a prescribed value and maintained for 15 min. Torque, temperature, load, and shaft speed were recorded at that time and load increased to the next value. The coefficient of friction was computed.

The coefficient of friction decreases in value with increased load as long as the bearing remains in the hydrodynamic mode. When the coefficient of friction

started increasing in value with increased load, signifying breakdown of the hydrodynamic film and entry into mixed lubrication region, the test was stopped. The bearings were removed for inspection and photographs were taken. The bearings were replaced in the machine and breakaway tests were then conducted.

For breakaway tests, the drive motor and torquemeter were disconnected because the expected static frictional torque exceeded their capacity. A torquewrench with a follower needle was used to manually conduct this test. Load was applied for time periods of 1 min, 5 min, 15 min, and 1 hour. The bulk oil temperature was maintained at 50°C (122°F). At the prescribed time, the shaft was rotated using the torquewrench. The needle follower on the scale indicated the highest torque reached to initiate rotation. This value was recorded. Load and time under load were increased until the limit of the torquewrench of 339 Nm (250 lb-ft) was reached.

An offset ratio of $x/B = 0.7$ was tested. Some preliminary testing with the swing-pad bearing showed that an offset of $x/B = 0.7$ produced the best results. The hybrid-pad bearing was expected to have similar performance to the swing-pad bearing; and, as such, $x/B = 0.7$ was adopted for it also. The coefficient of friction and the power losses for the tilt-pad bearing are relatively constant⁴ for x/B values ranging from 0.57 to 0.75. The minimum film thickness is reduced⁴ by 17 percent at $x/B = 0.7$. $x/B = 0.7$ was therefore used on this bearing as well as for uniformity.

BEARINGS TESTED

The swing-pad bearing was fabricated at DTNSRDC using a manufacturing technique developed and perfected with the assistance of the Center's rubber laboratory. The metallic components were fabricated in the machine shop.

The laminates consist of calendered sheets of Buna-N rubber vulcanized to the metal parts using a specially designed mold. The hardness of the cured rubber is 55 ± 5 on the Shore A scale. The mean radius of the laminates is 5.08 cm (2.00 in.). The bearing has four laminates. The pads were mounted 120 degrees apart on a 7.144 cm (2.813 in.) radius to center of pad. The surface area of the three pads is 26.5 cm^2 (4.1 in.²).

The tilt-pad bearing was purchased from Kingsbury Machine Works, Inc. It is a three-shoe, self-aligning, equalizing bearing with a radius to 6.668 cm (2.625 in.)

to the pivot point. The surface area of the three pads is 79.4 cm^2 (12.3 in.^2). The tilt-pad was first tested as received with the larger pad surface. Babbitt shoes identical to those used in the swing-pad were then bonded to the larger tilt-pad shoe (Figure 12) and tests were conducted as described. Frictional results of both arrangements were compared to data obtained in a shipboard application. The results agreed well in all cases. Therefore, it was concluded that no experimental error was being introduced by bonding smaller pad surfaces to the tilt-pad bearing assembly. The swing-pad and hybrid-pad bearing assemblies are shown in Figures 13 and 14, respectively. The spherical mating surfaces of the hybrid design were hardened to a value of 60 on the Rockwell C scale. The overall dimensions and the "swing" radius were identical to those of the swing-pad.

RESULTS

Test results are presented in Figures 15 through 21 and Tables 1 through 3. Figures 15 through 20 present the friction data of the dynamic tests for each bearing design. Figure 21 combines the curves of each of these tests for easier comparison. The coefficient of friction calculated from the torque measurements was plotted against the parameter $\mu U/PB$. These figures also include the theoretical curve which represents hydrodynamic conditions according to Equation (6).

The friction curves appear to have three distinct regions. The first is the region in which the experimental data are parallel to the predicted hydrodynamic behavior. The second region is characterized by departure from parallelism with the hydrodynamic curve, but undergoing minor changes in friction as bearing load increases. The third region is represented by abrupt changes in the friction coefficient with increased load. Each curve in Figures 15 through 20 are marked with the following symbols: o, representing the last condition indicative of hydrodynamic behavior; and , representing the last transition point before the onset of a sudden increase in the coefficient of friction as load is increased. Data under these conditions are used as a basis of comparison for each of the bearing designs and are used in Tables 1 and 2. The load at the point marked with symbol o is referred to as the "hydrodynamic load capacity," because it represents the highest load obtained under hydrodynamic conditions. Breakaway friction coefficients under 2,950 kPa (428 psi) are presented in Table 3.

TABLE 1 - LAST HYDRODYNAMIC VALUES

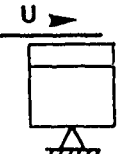

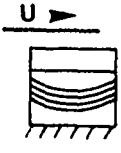
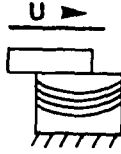
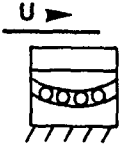
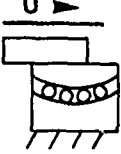
Bearing Description	$\mu U/PB$	f, Coefficient of Friction	h_o , Calc $\mu m(in.)$	P, Calc kPa(psi)	Figure
Centered Tilt-Pad 	8.6×10^{-8}	0.00102	2.5 (9.7×10^{-5})	3,923 (569)	15
Offset Tilt-Pad 	4.3×10^{-8}	0.00078	1.8 (6.8×10^{-5})	7,853 (1,139)	16
Centered Swing-Pad 	6.8×10^{-8}	0.00110	2.2 (8.6×10^{-5})	4,964 (720)	17
Offset Swing-Pad 	5.2×10^{-8}	0.00098	1.9 (7.5×10^{-5})	6,495 (942)	18
Centered Hybrid-Pad 	4.8×10^{-8}	0.00094	1.8 (7.2×10^{-5})	7,033 (1,020)	19
Offset Hybrid-Pad 	5.5×10^{-8}	0.00088	1.9 (7.7×10^{-5})	6,136 (890)	20

TABLE 2 - LAST TRANSITION ZONE VALUES FROM
HYDRODYNAMIC TO MIXED LUBRICATION





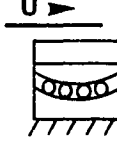
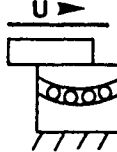
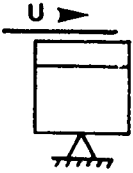
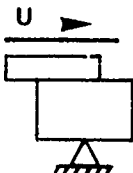
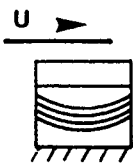
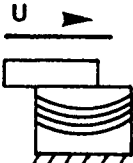
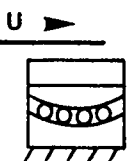
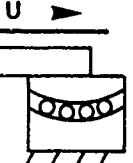
Bearing Description	$\mu U/PB$	f, Coefficient of Friction	P, Calc kPa(psi)	Figure
Centered Tilt-Pad 	2.9×10^{-8}	0.00096	11,638 (1,688)	15
Offset Tilt-Pad 	1.6×10^{-8}	0.00086	21,098 (3,060)	16
Centered Swing-Pad 	2.8×10^{-8}	0.00145	12,059 (1,749)	17
Offset Swing-Pad 	1.2×10^{-8}	0.00093	28,131 (4,080)	18
Centered Hybrid-Pad 	1.7×10^{-8}	0.00120	19,857 (2,880)	19
Offset Hybrid-Pad 	1.6×10^{-8}	0.00090	21,098 (3,060)	20

TABLE 3 - BREAKAWAY COEFFICIENT OF FRICTION

Bearing Description	Average Breakaway Coefficient of Friction under 2,950 kPa (428 psi)
<p>Centered Tilt- Pad</p> 	0.20
<p>Offset Tilt- Pad</p> 	0.15
<p>Centered Swing- Pad</p> 	0.30
<p>Offset Swing- Pad</p> 	0.29
<p>Centered Hybrid- Pad</p> 	0.19
<p>Offset Hybrid- Pad</p> 	0.18

DISCUSSION

Frictional results presented in Figures 15 through 20 show that all bearings exhibited behavior characteristic of hydrodynamic conditions for higher values of $\mu U/PB$. Note that, for each bearing design, the magnitude of the friction coefficient is higher than that predicted by theory. This is expected because the measured torque contains not only the shear losses predicted by theory in the lubricant film but also the drag of the rotating parts in the oil reservoir and the turbulence between the pads. The friction predicted is also dependent upon the ratio of inlet film thickness to minimum film thickness. The intent of the theoretical friction curve is to provide a reference to determine the type of lubrication existing under various test conditions.

Table 1 lists the coefficient of friction and value of $\mu U/PB$ from Figures 15 through 20 for the last point indicative of hydrodynamic conditions. From the test parameters μ , U , and B , the value of h_o is calculated for each design using Equation (7) as follows:

$$h_o = 0.264 \left[\left(\frac{\mu U}{PB} \right) (B^2) \right]^{1/2}$$

The load P is calculated from the value $\mu U/PB$, because it did not always correspond to a data point where the load was known. The maximum load under hydrodynamic conditions for the centered swing-pad and centered hybrid-pad bearings were increased by 25 and 80 percent respectively, compared with the centered tilt-pad bearing. Improvements in the hydrodynamic region were observed when the pad surfaces were offset to $x/B = 0.7$ for the tilt-pad and laminated elastomer swing-pad, but not the hybrid-pad. It is suspected that the optimum offset for the hybrid-pad is probably much closer to the center because it does not require as much offset moment to cause wedge formation. The constraints limiting extension of hydrodynamic behavior appear to be the film thickness.^{9,10,11,12} Calculated minimum film thicknesses from Table 1 range from 1.8 to 2.5 μm (0.75 to 0.97 $\mu in.$) Metal-to-metal contact initiates when the lubricant film thickness is about 10 times the order of rms surface finish.¹¹ The average surface roughness of the runner in the direction of motion is 0.15 μm rms (0.063 $\mu in.$). The expected limit¹¹ is therefore 1.5 μm rms (0.63 $\mu in.$), which is close to the values calculated from the experiment.

The transition region from hydrodynamic behavior to the point at which the coefficient increases abruptly with increased load is extended in all designs by offsetting the pad surfaces (see Figure 21).

The coefficient of friction for the breakaway tests were unaffected by the time under load. The values in Table 3 were obtained by averaging results of the four tests; 1 min, 5 min, 15 min, and 1 hour under load. The friction coefficients of the tilt-pad and hybrid-pad are about the same. The coefficient of friction of the swing-pad bearing is about 50 percent higher. Offsetting of the surface did not affect the breakaway friction of any design.

Frictional results of this report did not agree with expectations based on a previous report¹ for either the dynamic or breakaway experiments even though the same basic size and design swing-pad bearing was used. It is suspected that the type of conventional bearing used for comparison in the previous report did not represent its characteristic behavior.

CONCLUSIONS

Based upon a single series of tests on each of the six bearing designs, the following conclusions are made:

- (1) Below bearing unit loads of 3,900 kPa (569 psi), all bearing designs exhibited behavior characteristic of hydrodynamic conditions.
- (2) The limit for hydrodynamic behavior appears to be more dependent upon the surface finish of the runner surface than upon bearing design.
- (3) The maximum load under hydrodynamic conditions for the centered swing-pad and centered hybrid-pad were increased by 25 and 80 percent respectively, compared to the tilt-pad bearing.
- (4) Improvements in hydrodynamic performance of both the tilt-pad and laminated elastomeric swing-pad bearing were observed by offsetting the pad surfaces.
- (5) The transition region from hydrodynamic behavior to the point at which the coefficient of friction increases abruptly with increased load is extended in all designs by offsetting the pad surfaces.
- (6) Variation in time of 1 to 60 min under a load of 2,950 kPa (428 psi) did not affect the breakaway friction of any design.
- (7) The breakaway coefficient of friction of the laminated elastomeric swing-pad bearing was about 50 percent higher than that measured for either the conventional tilt-pad or hybrid-pad bearing.

(8) Offsetting the pad surfaces did not affect the breakaway friction of any design.

FUTURE PLANS

No further experimental evaluation of the swing-pad bearing designs is planned. Efforts have been focused upon development of a model for the swing-pad bearing so that the design can be optimized. The tests described in this report were based primarily upon previous test results.¹ There are several parameters which appear to affect the performance of the swing-pad, such as the amount of offsetting of the center of swing compared with the center of the pad, the radius of curvature of the laminates, and the compressive and shear stiffness. An in-house effort is underway in FY 80 to develop such a mathematical model. If successful and if optimization looks promising, additional experiments will be needed to verify such expectations.

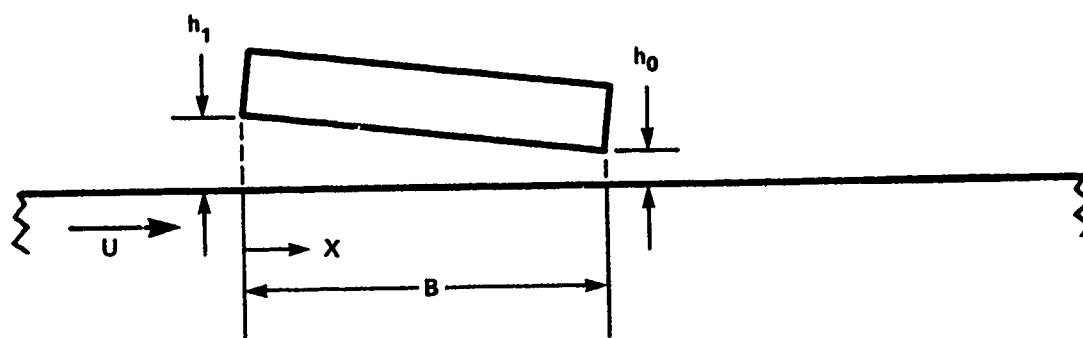


Figure 1 - Hydrodynamic Converging Tapered Wedge

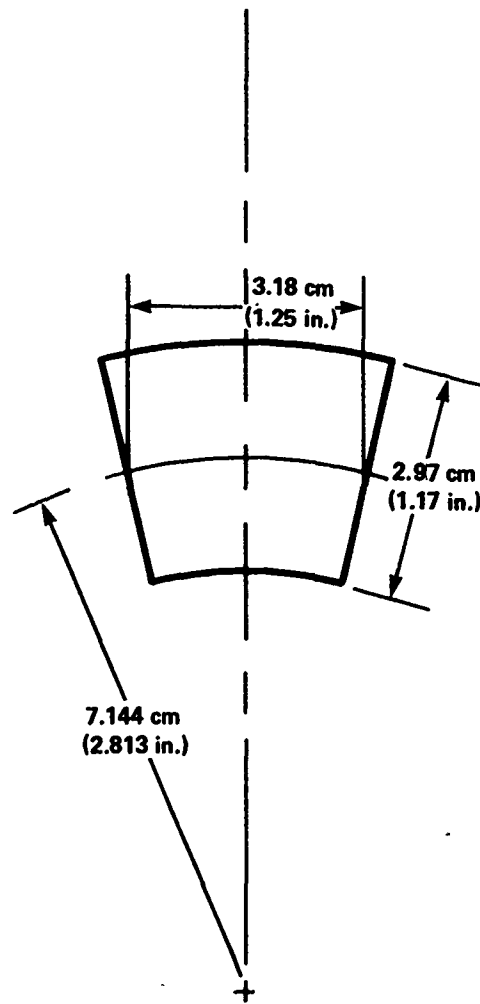


Figure 2 - Shoe Dimensions

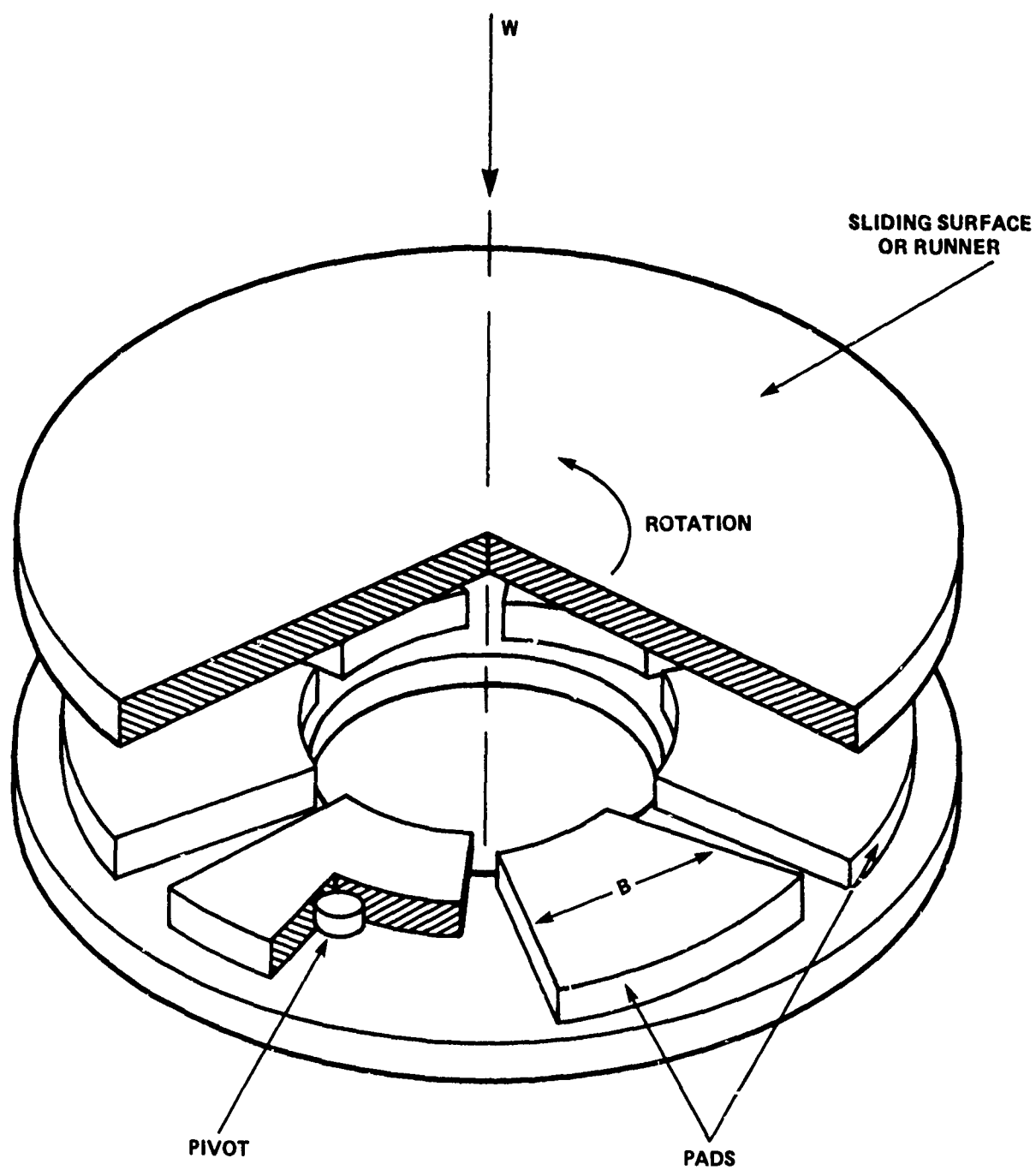


Figure 3 - Typical Tilt-Pad Thrust Bearing Assembly

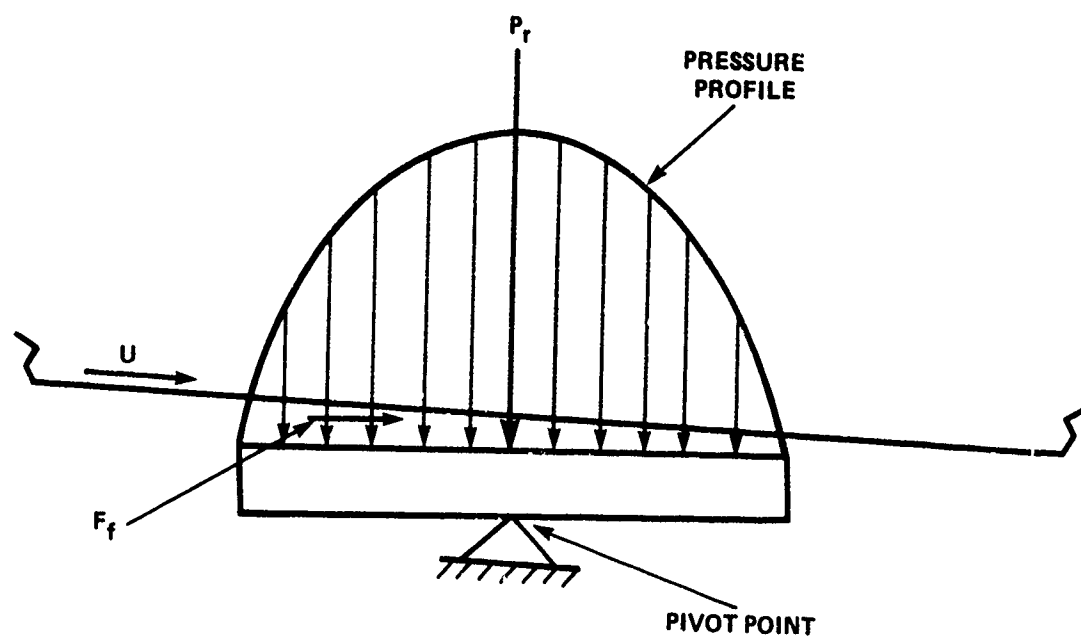


Figure 4 - Pressure Distribution on Tilt-Pad Bearing

- 1 CENTER OF SWING
- 2 SWING RADIUS
- 3 BABBITT SURFACE
- 4 SURFACE PLATFORM
- 5 ELASTOMER LAMINATES
- 6 MOUNTING BASE
- 7 METAL SHIMS

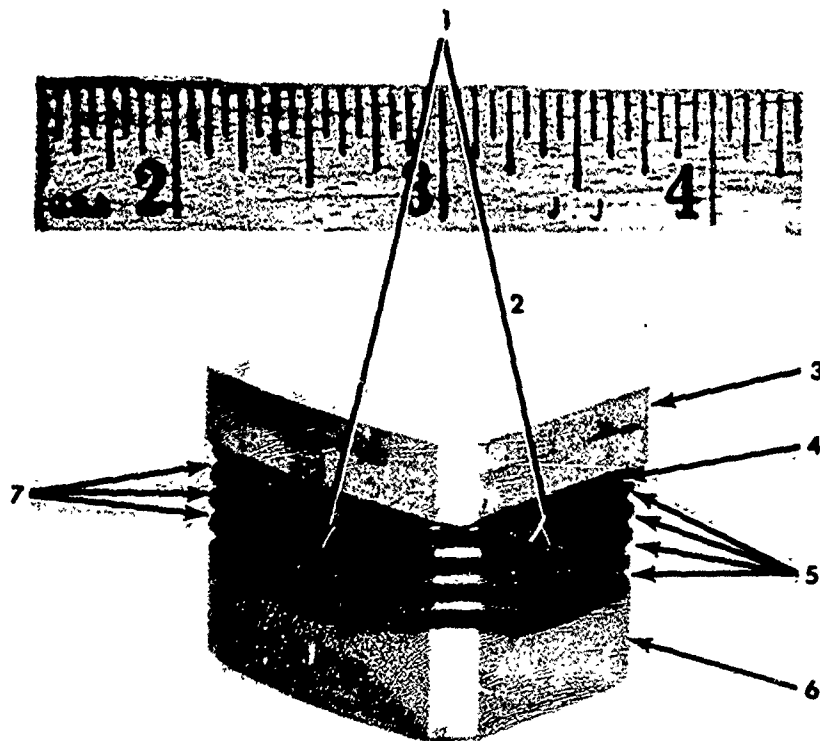


Figure 5 - Swing-Pad Bearing, Centered

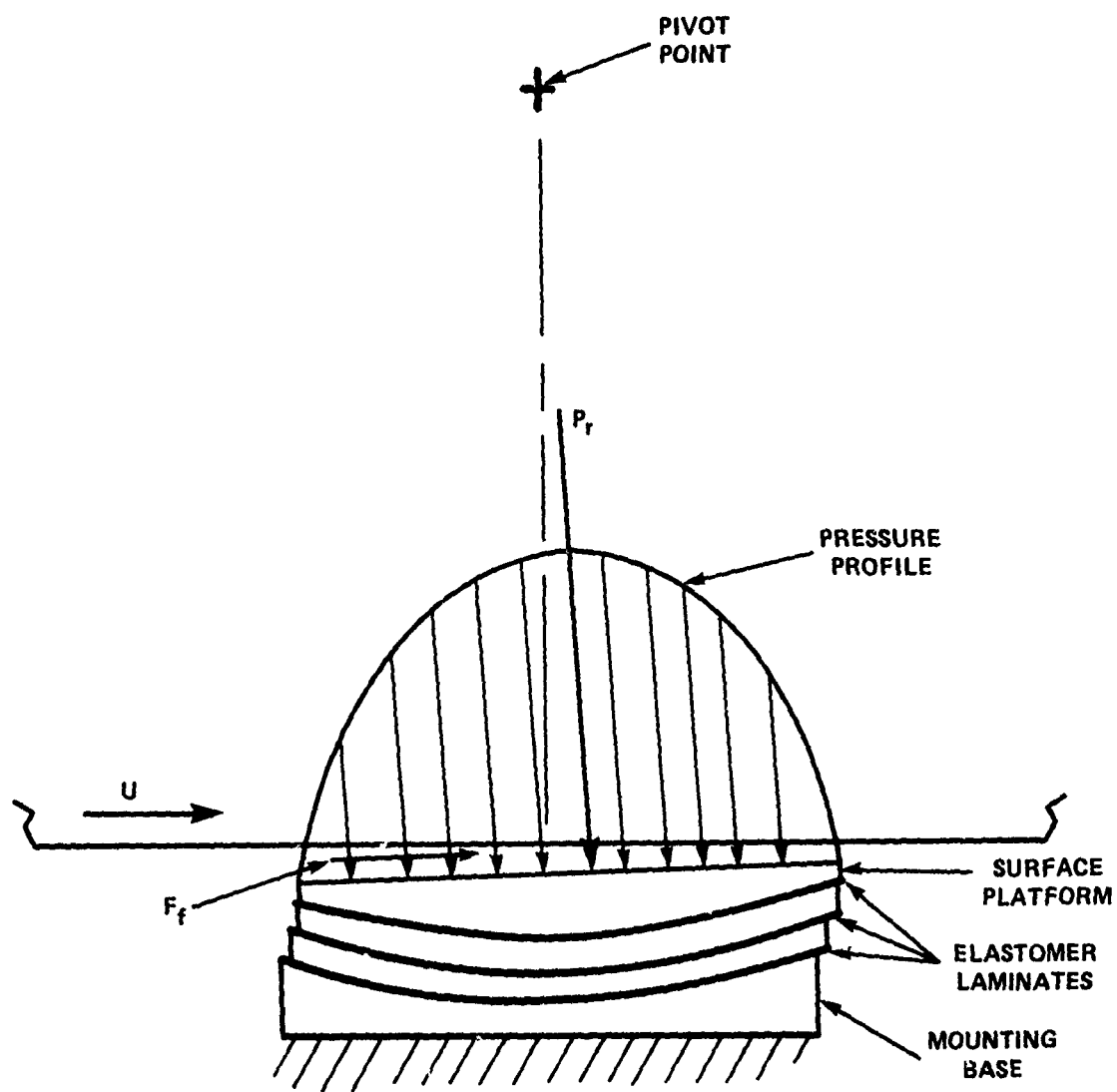


Figure 6 - Pressure Distribution of Swing-Pad Bearing

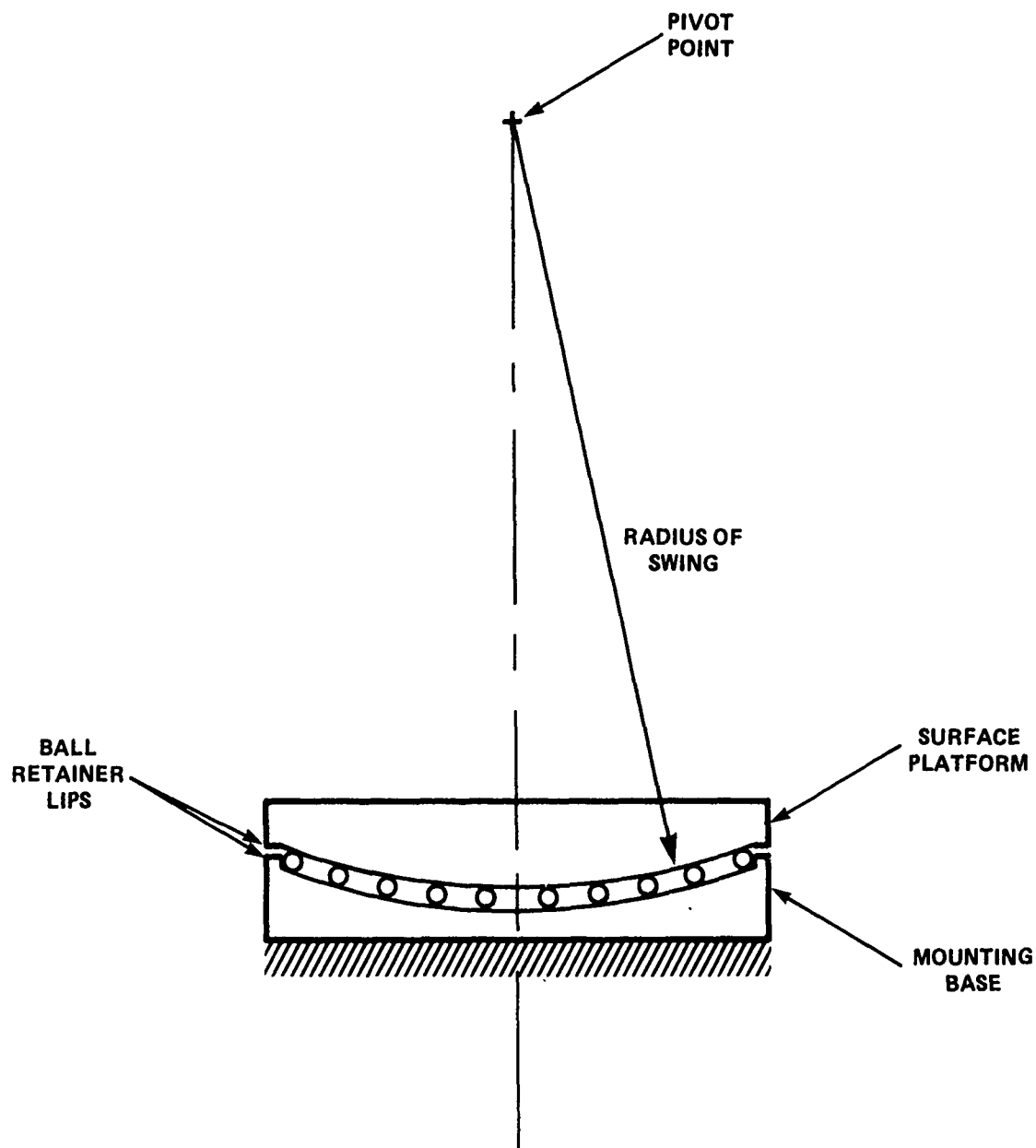


Figure 7 - Hybrid-Pad Bearing

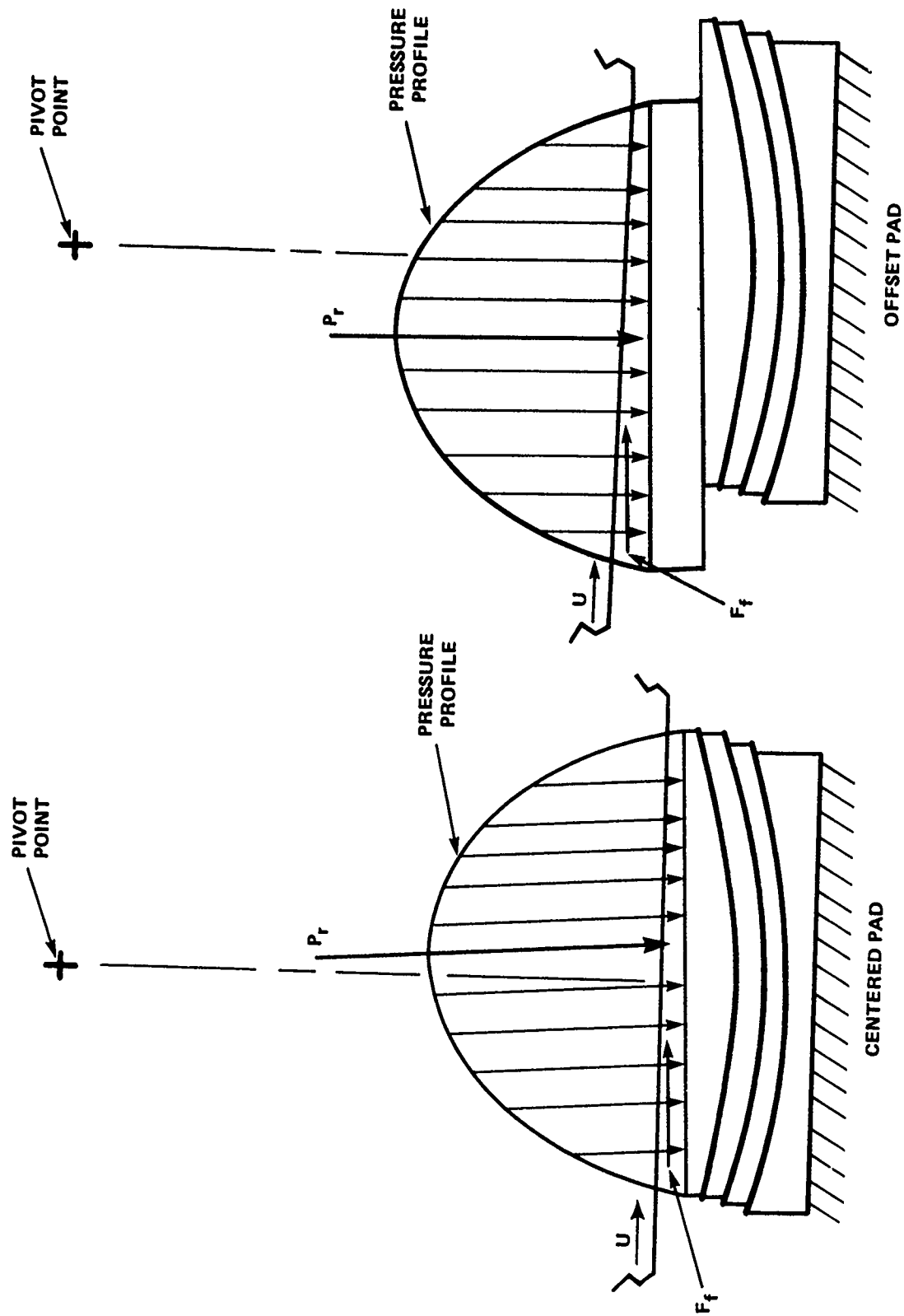


Figure 8 - Centered and Offset Swing-Pad Bearing

- 1 HYDRAULIC MOTOR
- 2 REDUCTION GEAR
- 3 TORQUE SENSOR
- 4 OIL TANK
- 5 LOAD PISTON BLOCKS
- 6 HEATER

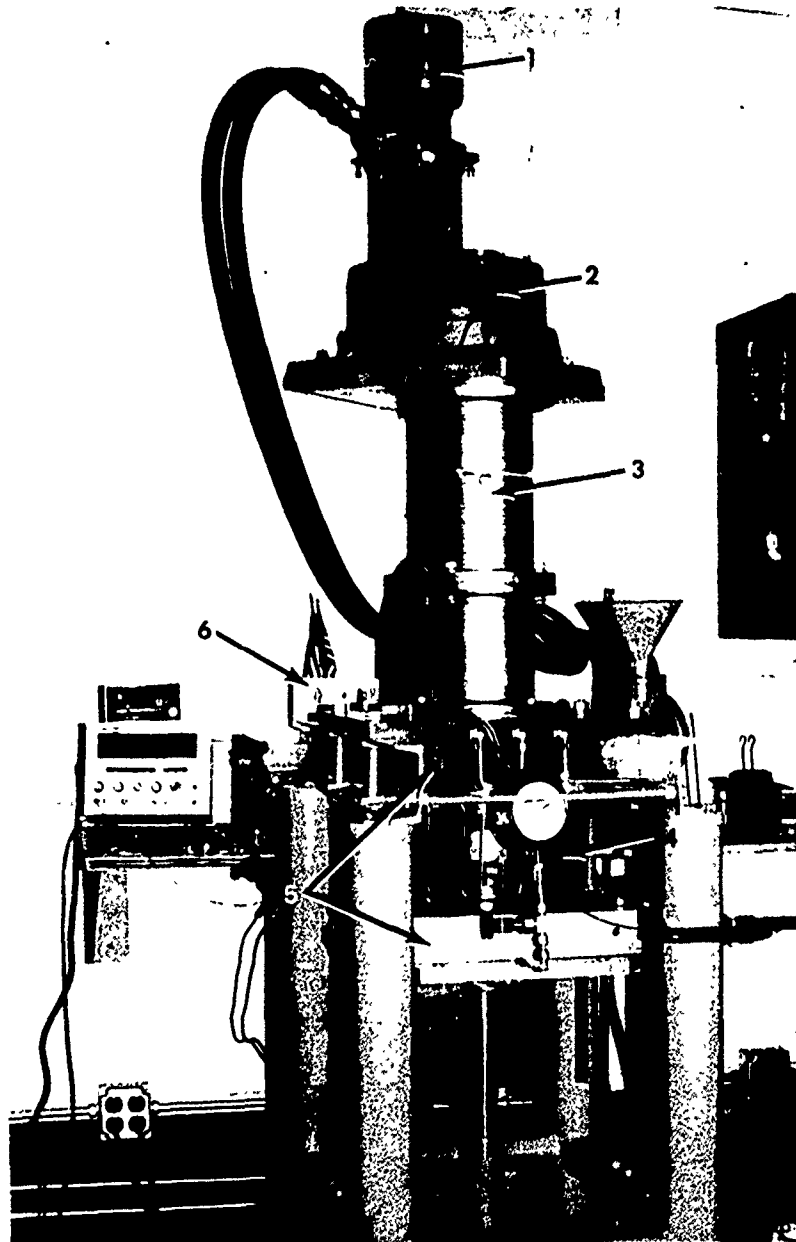


Figure 9 - Test Machine

- 1 HEATING COIL
- 2 RUNNER PLATES
- 3 TEST BEARING
- 4 THERMOCOUPLE

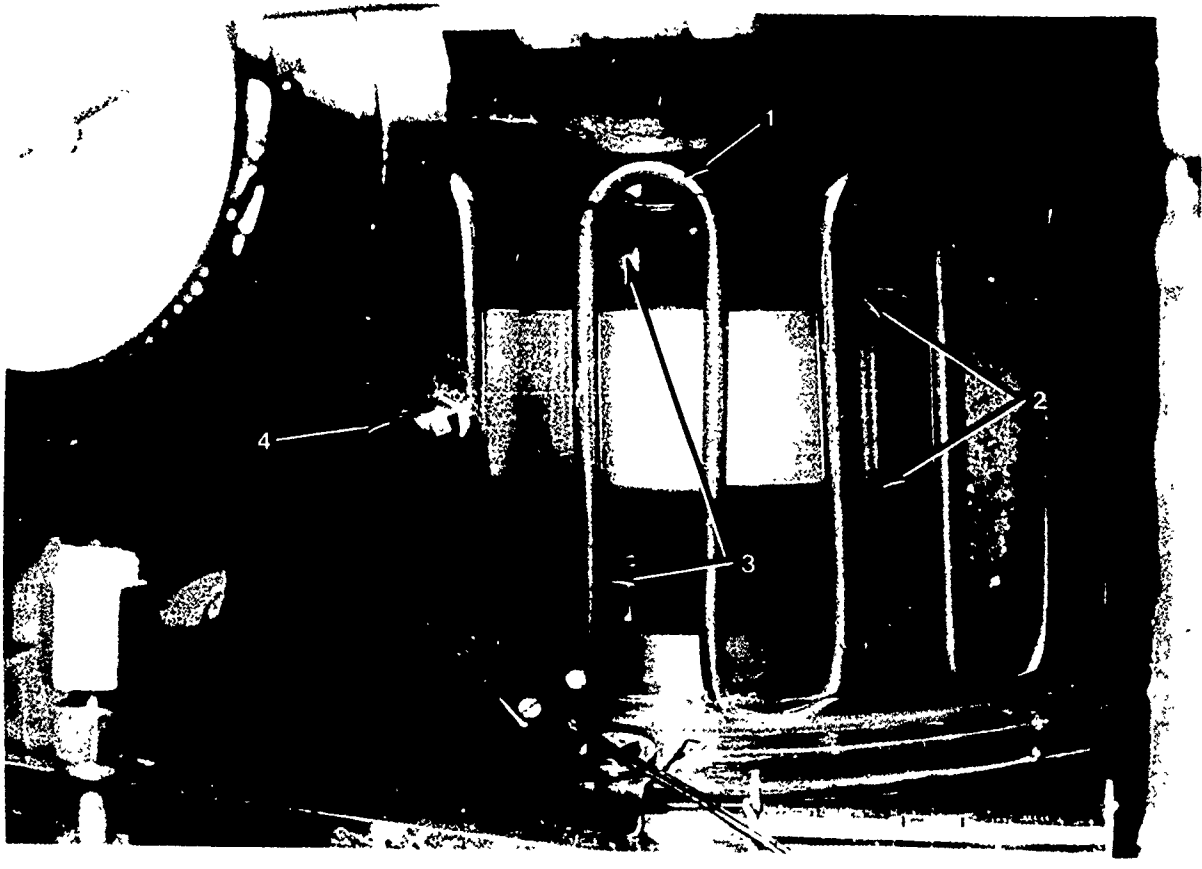


Figure 10 - Test Bearing in Oil Tank

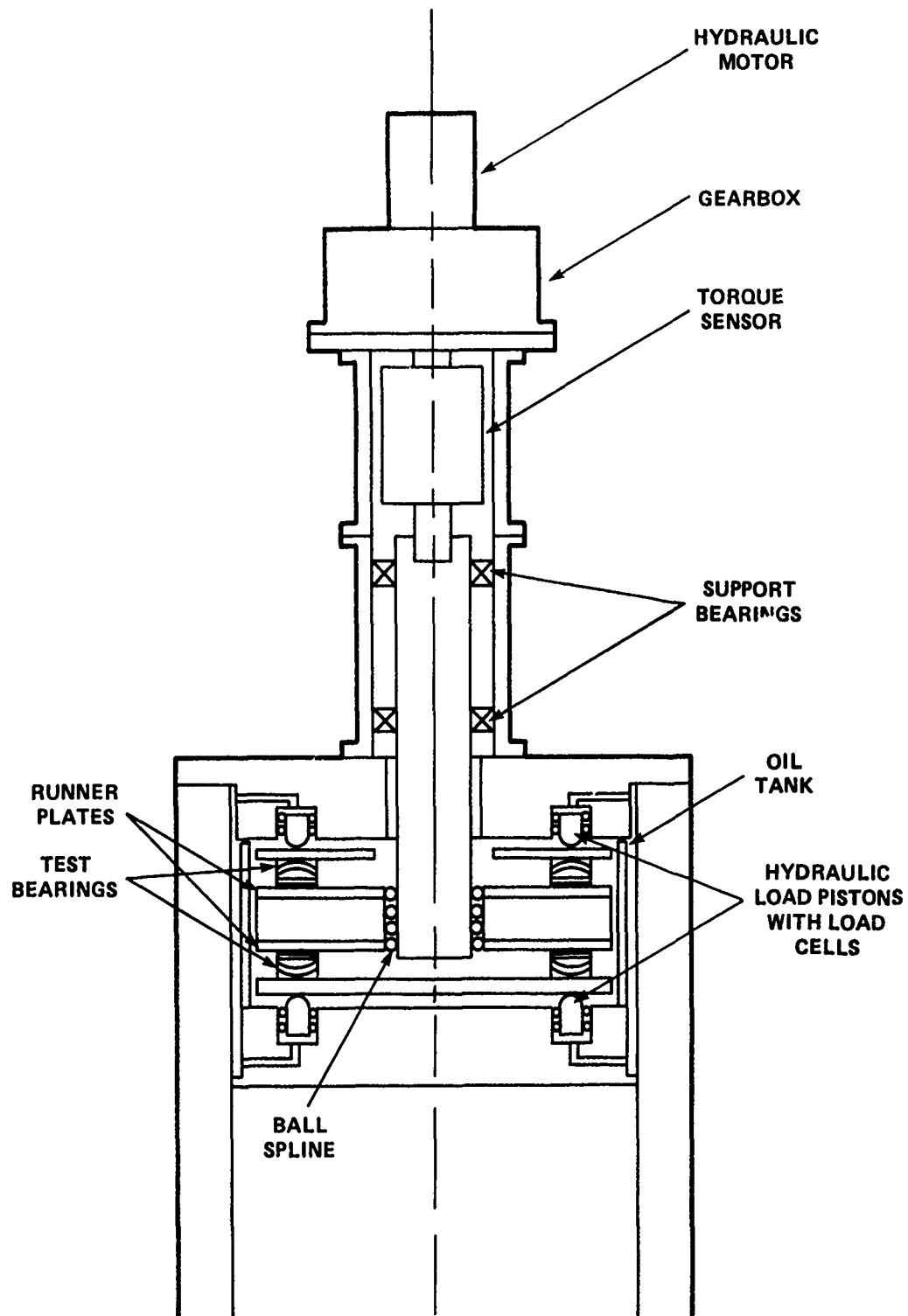


Figure 11 - Test Machine Schematic

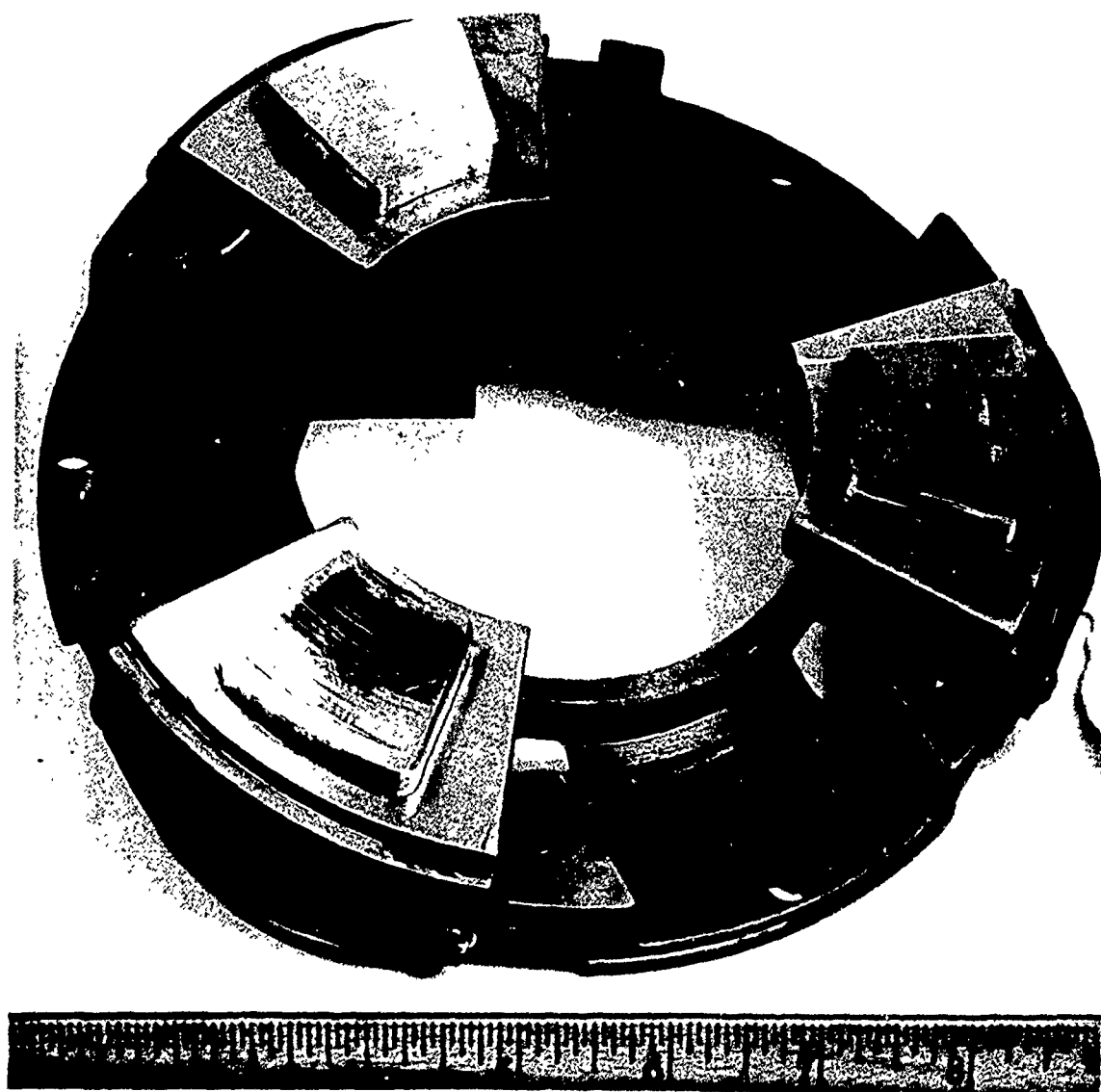


Figure 12 - Tilt-Pad Assembly, Centered (After Test)

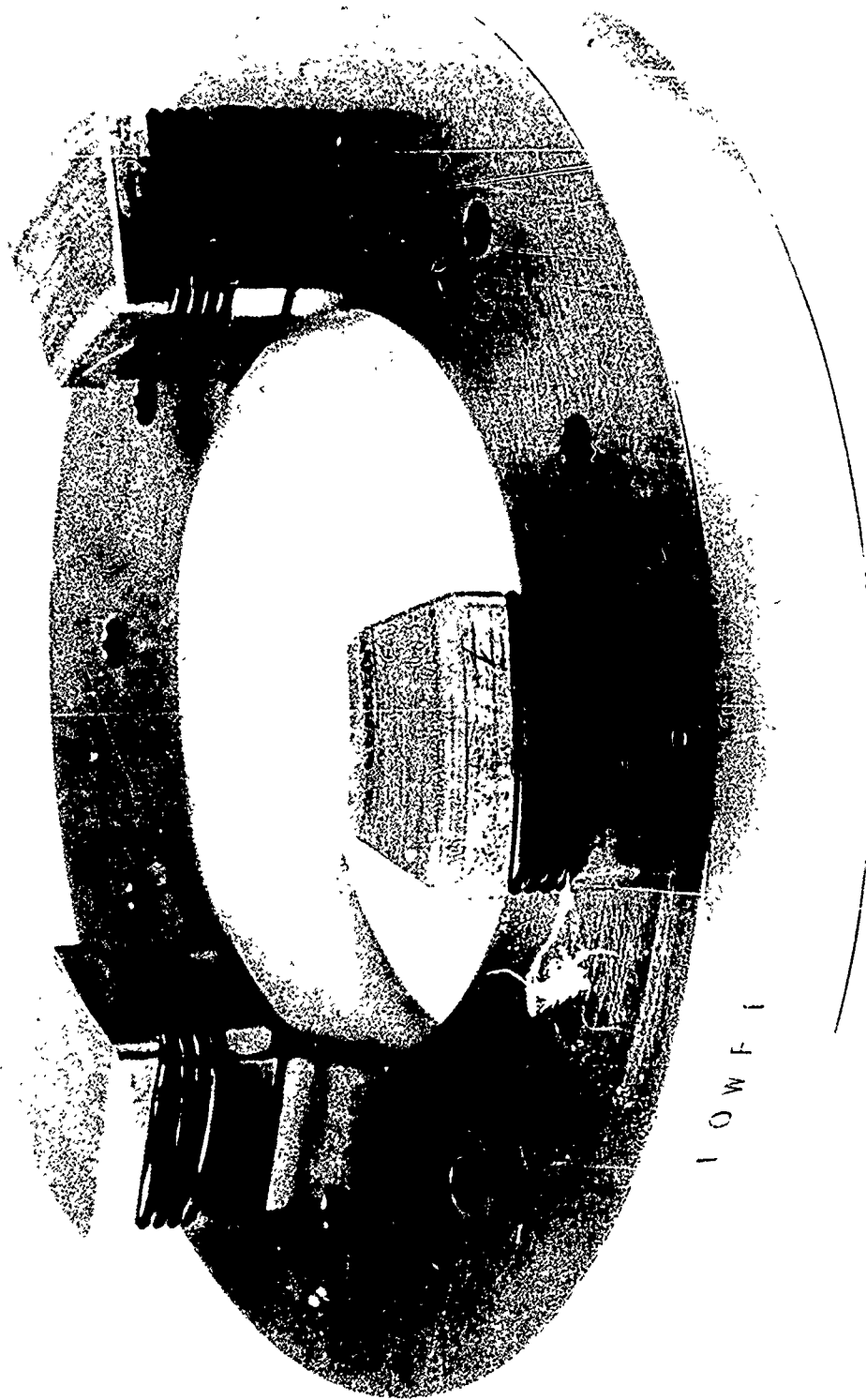


Figure 13 - Swing-Pad Assembly, Centered

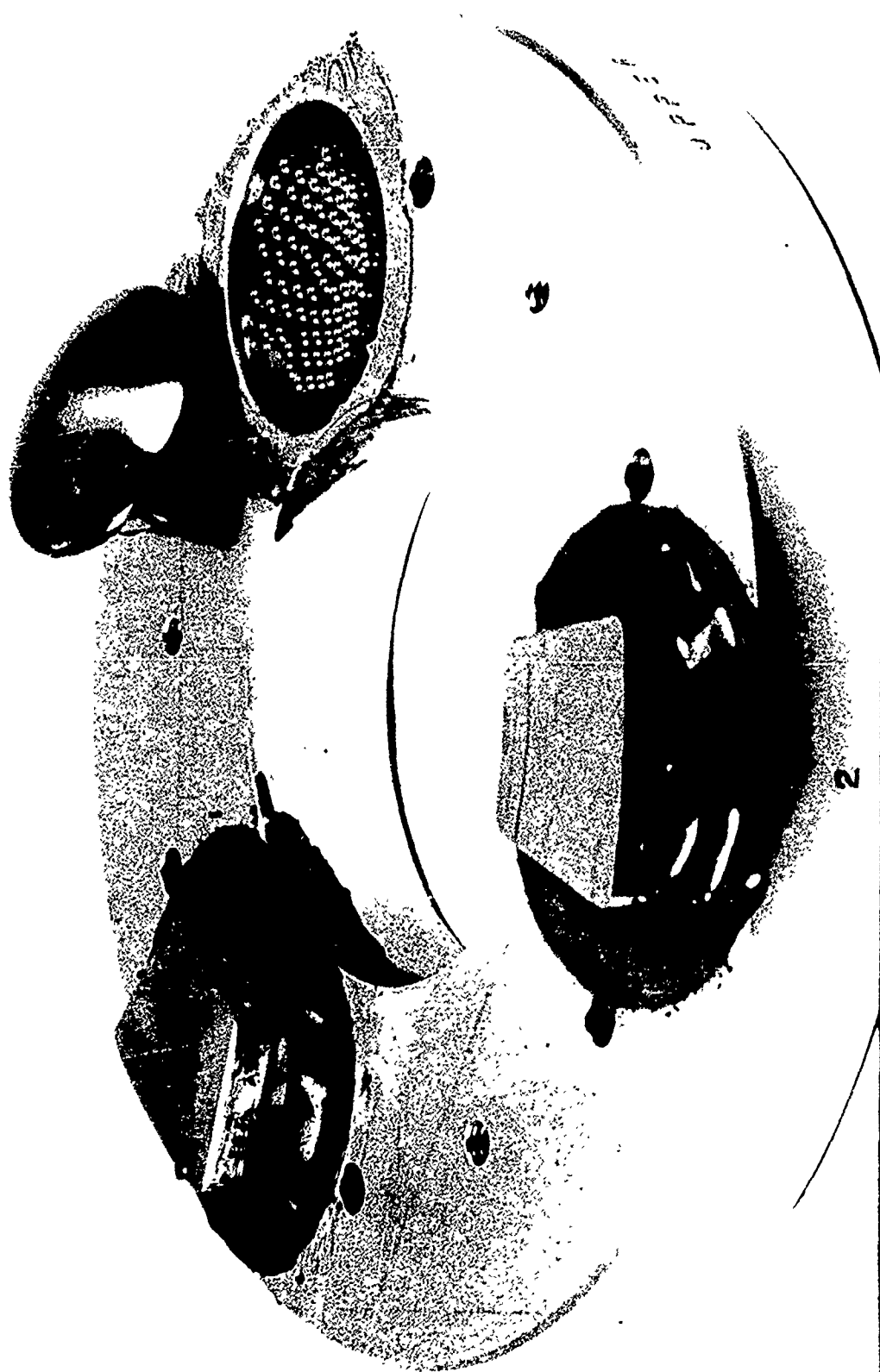


Figure 14 - Hybrid-Pad Assembly, Centered

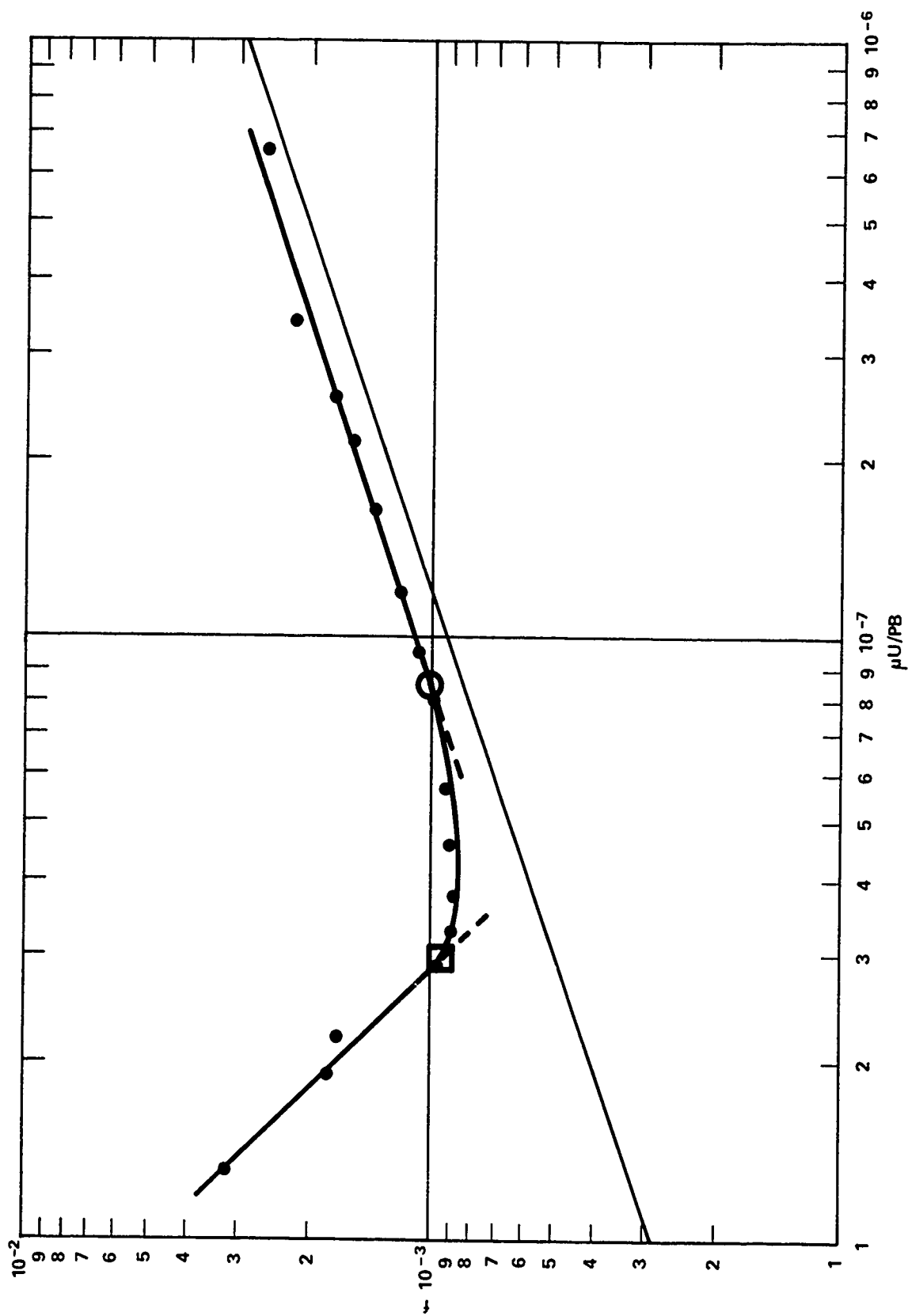


Figure 15 - Results, Tilt-Pad, Centered

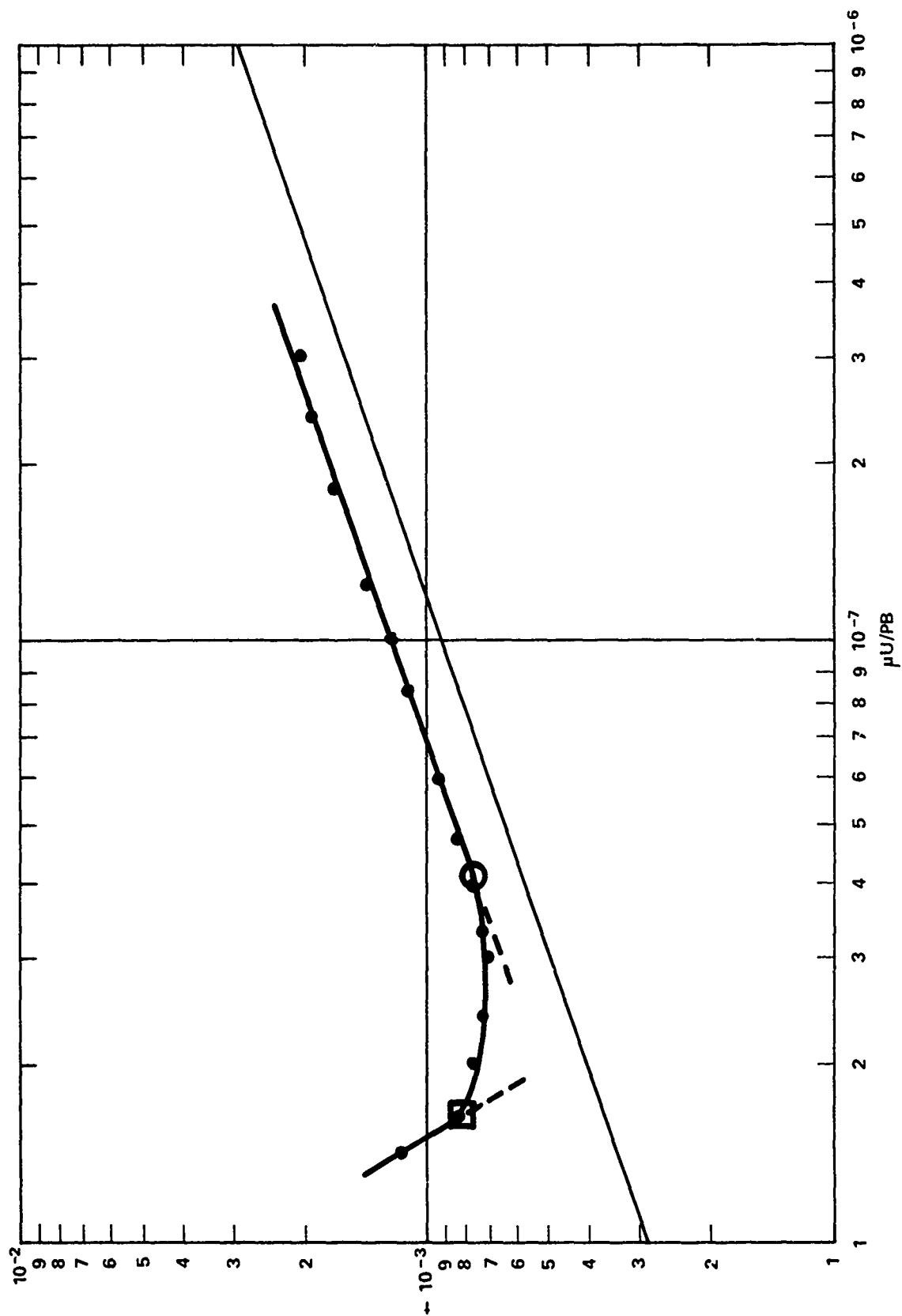


Figure 16 - Results, Tilt-Pad, Offset

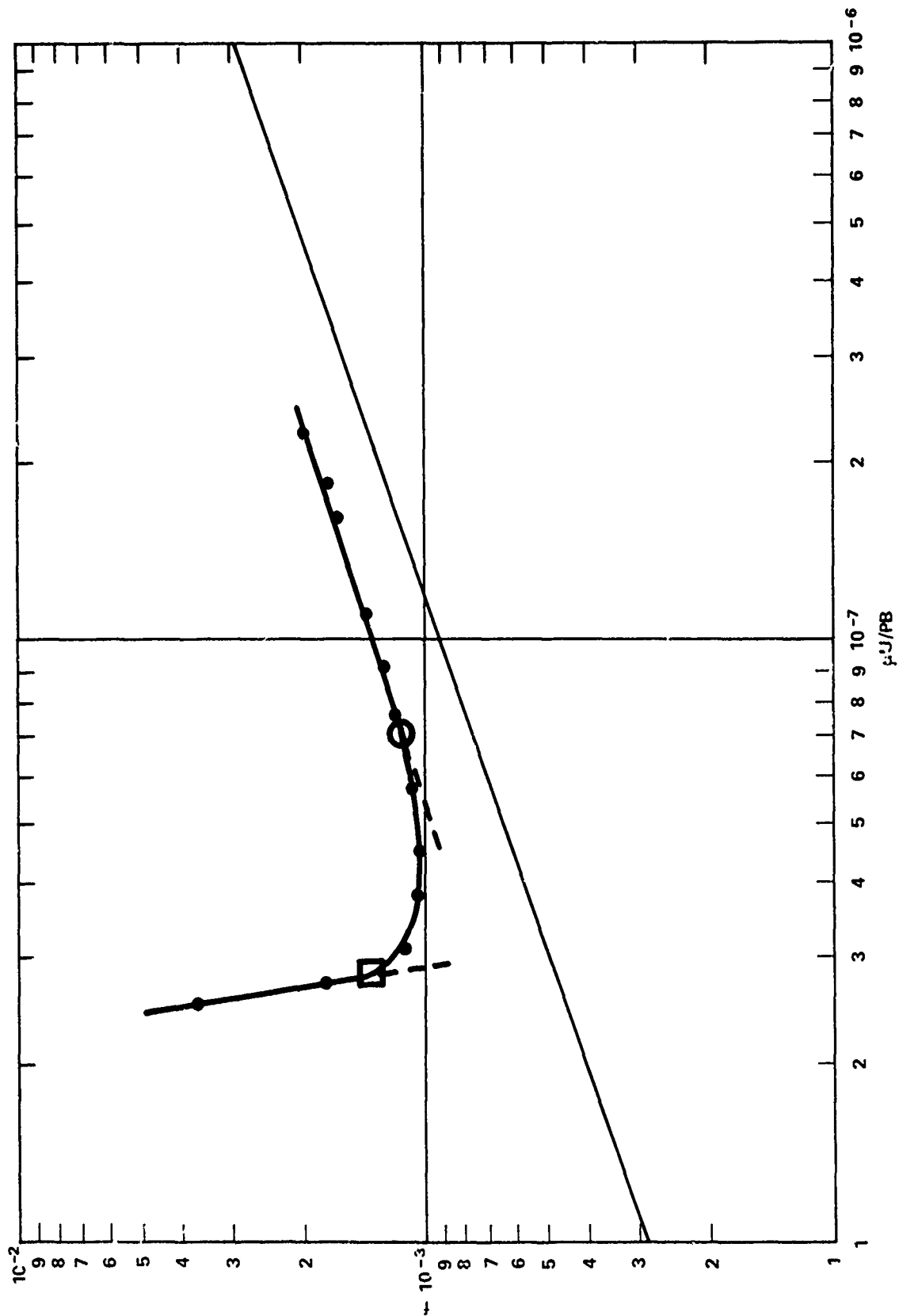


Figure 17 - Results, Swing-Pad, Centered

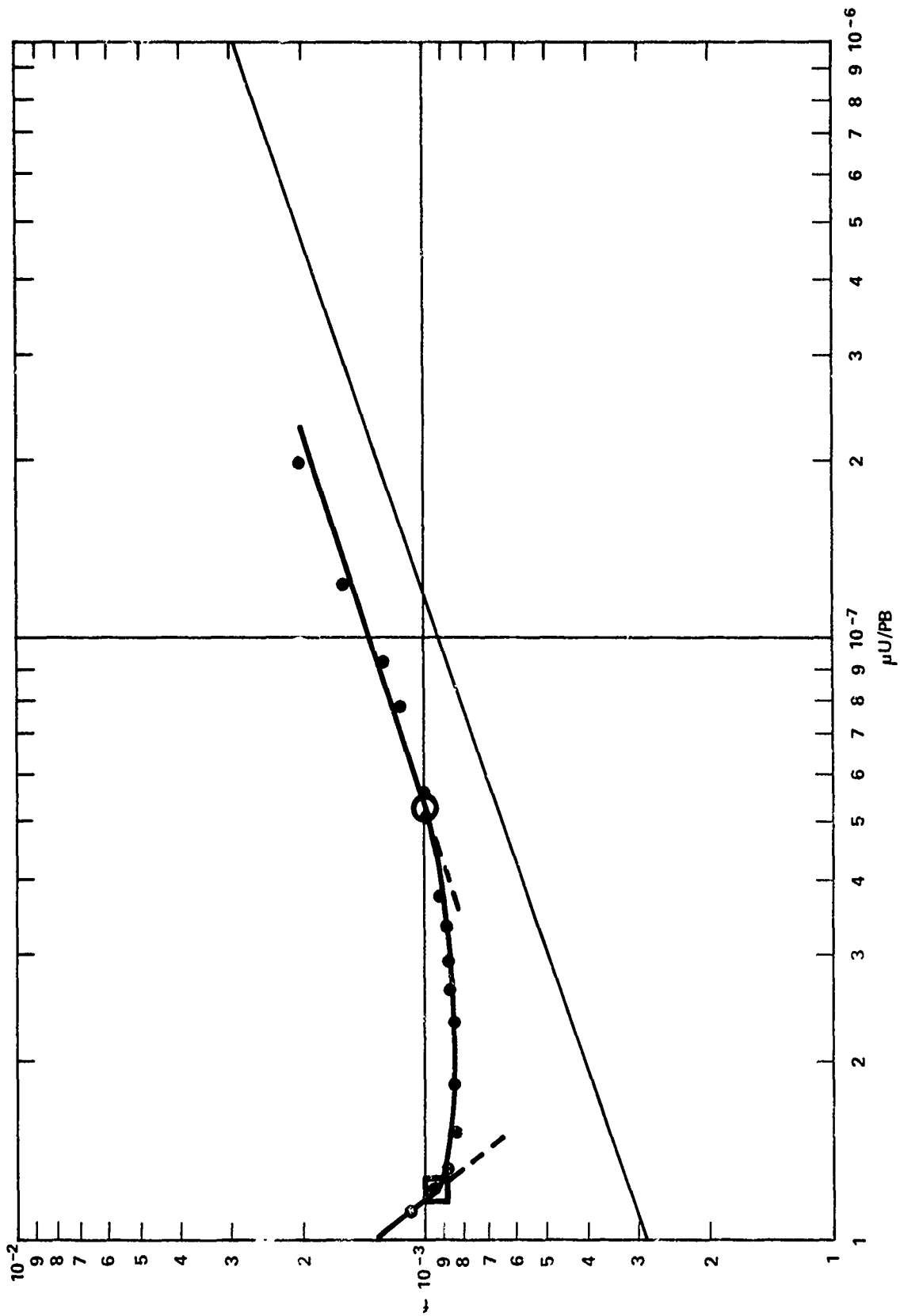


Figure 18 - Results, Swing-Pad, Offset

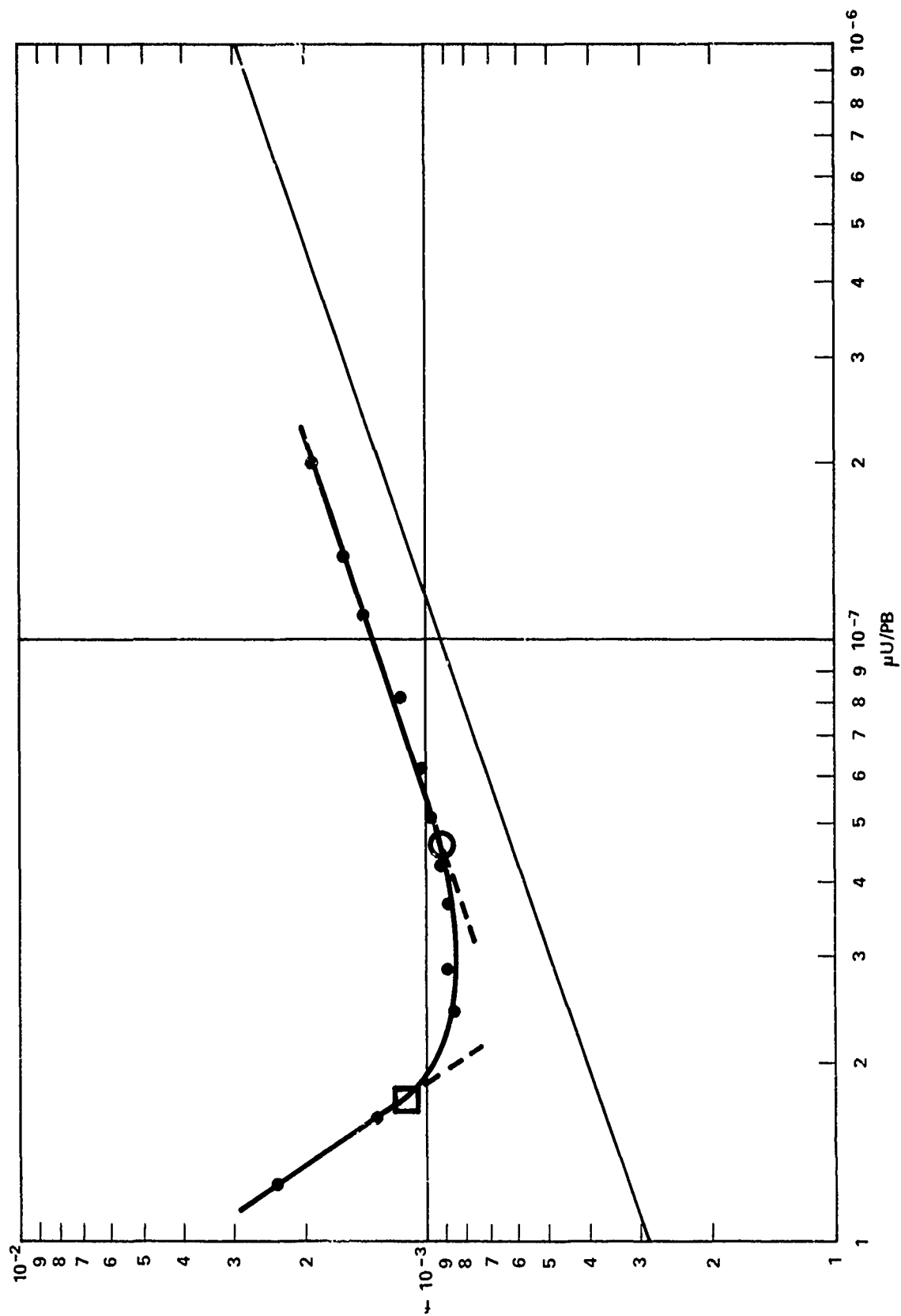


Figure 19 - Results, Hybrid-Pad, Centered

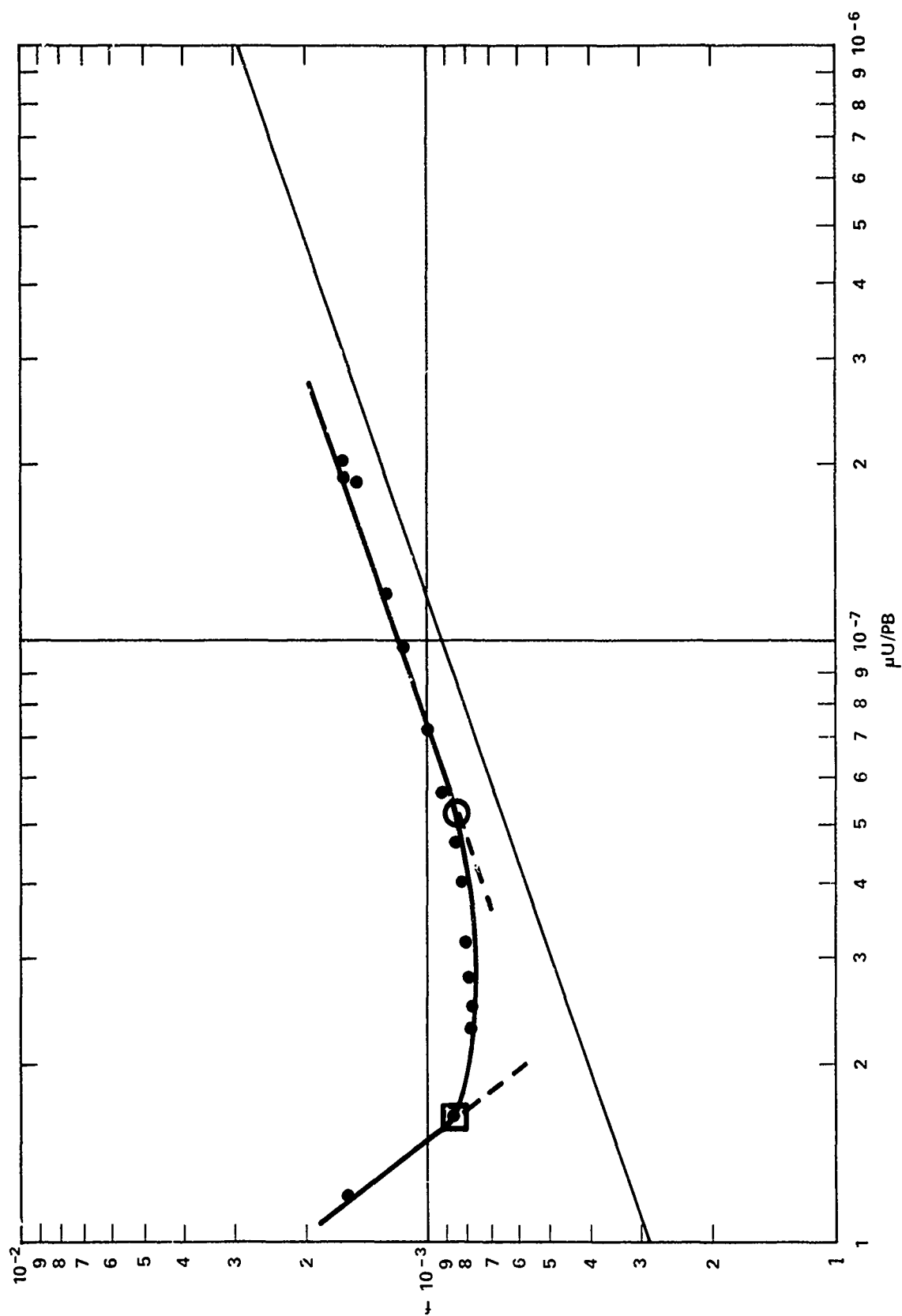


Figure 20 - Results, Hybrid-Pad, Offset

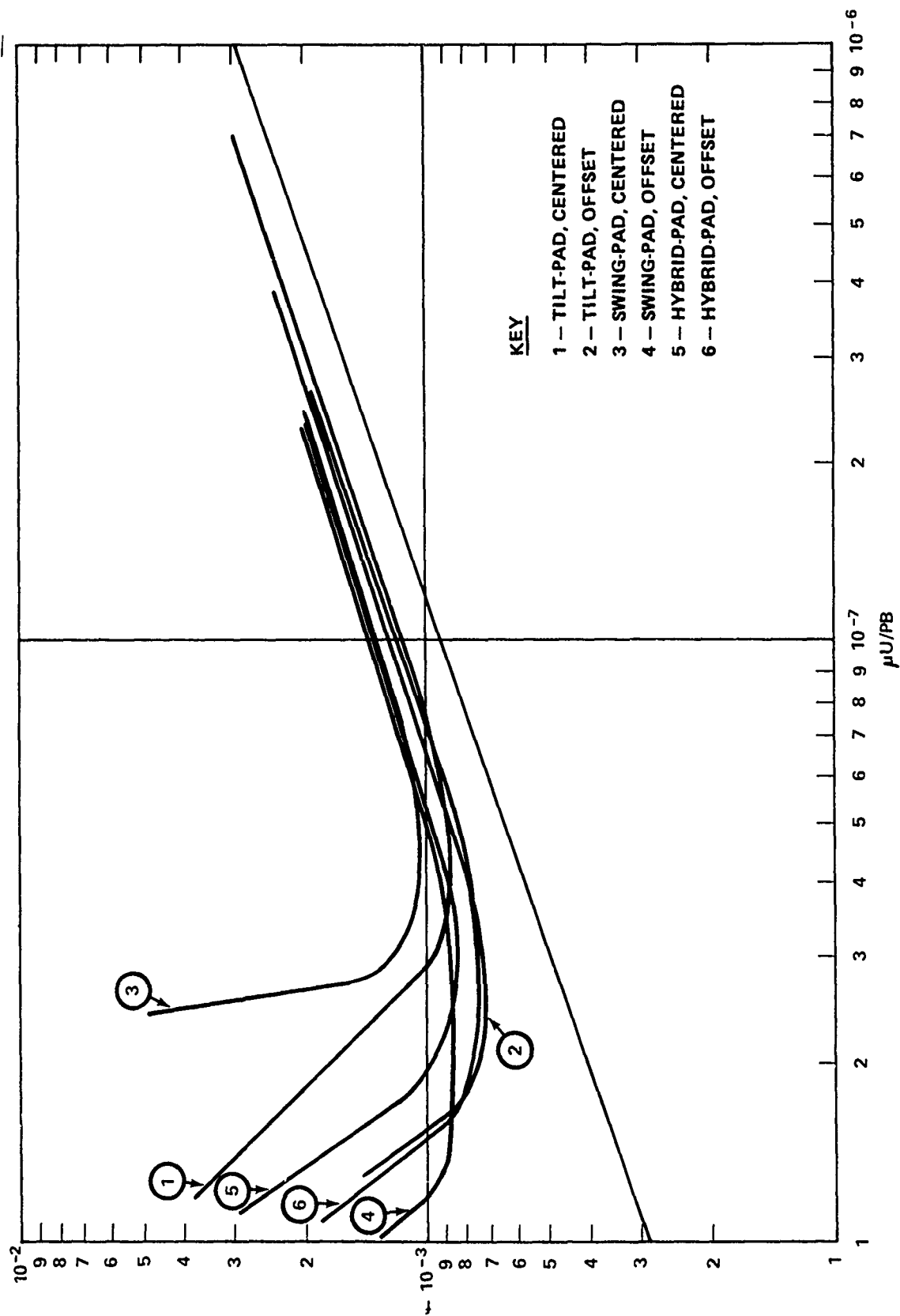


Figure 21 - Superimposed Plots

REFERENCES

1. Greene, J., "The Swing-Pad Bearing - A New Concept in Sliding-Surface Bearings," DTNSRDC Report 76-0055 (Dec 1976).
2. Fuller, Dudley D., "Theory & Practice of Lubrication for Engineers," John Wiley & Sons, Inc. (1955).
3. Cameron, Alastair, "Basic Lubrication Theory," 2nd Ed., Ellis Horwood Ltd. (1976).
4. Raimondi, A.A. and John Boyd, "Applying Bearing Theory to the Analysis and Design of Pad-Type Bearings," Transactions of the ASME (Apr 1955).
5. Pinkus, O. and B. Sternlicht, "Theory of Hydrodynamic Lubrication," McGraw-Hill, N.Y. (1961).
6. Raimondi, A.A. and John Boyd, "The Influence of Surface Profile on the Load Capacity of Thrust Bearings with Centrally Pivoted Pads," Transactions of the ASME (Apr 1955).
7. Hersey, Mayo Dyer, "Theory and Research in Lubrication," J. Wiley & Sons, Inc., New York (1966).
8. "Standard Handbook of Lubrication Engineering," J.J. O'Connor and J. Boyd, Editors, McGraw-Hill Co. (1968) p. 5-23 ff.
9. Kreisle, L.F., "Predominant-Peak Surface Roughness, a Criterion of Minimum Hydrodynamic Oil-Film Thickness of Short Journal Bearings," Transactions of the ASME (Aug 1957).
10. Ledocq, H.M., "The Transition from Hydrodynamic to Boundary Regime of Tilting-Thrust Pads," Tribology (Feb 1974).
11. Elwell, R.C. and E.R. Booser, "Low Speed Limit of Lubrication," Machine Design (15 Jun 1972).
12. Gardner, W.W., "Journal Bearing Operation at Low Sommerfeld Numbers," ASLE Transactions, Vol. 19, 3, pp 187-194.

INITIAL DISTRIBUTION

Copies

9 NAVSEA
 1 SEA 05
 3 SEA 05DC
 1 SEA 05R
 1 SEA 052
 1 SEA 524
 2 SEA 99612

12 DTIC

Copies	Code	Name
4	1102	R.M. Stevens
2	272	Dr. Quandt
1	2723	Mr. Strucko
1	283	Dr. Bosmajian
24	2832	T.L. Daugherty
10	5211.1	Rept Distribution
1	522.1	Class Lib (C)
1	522.2	Class Lib (A)

DISCLAIMER NOTICE

THIS DOCUMENT IS BEST QUALITY PRACTICABLE. THE COPY FURNISHED TO DTIC CONTAINED A SIGNIFICANT NUMBER OF PAGES WHICH DO NOT REPRODUCE LEGIBLY.